Photochemical Characterization of a Novel Fungal Rhodopsin from *Phaeosphaeria nodorum*

Ying Fan[a], Peter Solomon[b], Richard P. Oliver[c], Leonid S. Brown[a,*]

[a]Department of Physics and Biophysics Interdepartmental Group, University of Guelph, Ontario, Canada, N1G 2W1; [b]Research School of Biology, College of Medicine, Biology and the Environment, The Australian National University, Canberra ACT 0200, Australia; [c]Australian Centre for Necrotrophic Fungal Pathogens, Department of Environment and Agriculture, Curtin University, GPO Box U1987, Perth, WA 6102, Australia

[*]Correspondence should be addressed to L.S. Brown (leonid@physics.uoguelph.ca), fax: 1(519)836-9967

Keywords: photosensory transduction, membrane proteins, fungal rhodopsins, retinal proteins, photochemical cycle, proton pumping

[1]Abbreviations: RDs – rhodopsins; ORPs – opsin-related proteins; BR – bacteriorhodopsin; LR – *Leptosphaeria* rhodopsin; NR – *Neurospora* rhodopsin; PhaeoRD1 – LR-like rhodopsin from *Phaeosphaeria*; PhaeoRD2 – the second (auxiliary) rhodopsin from *Phaeosphaeria*; PCR – polymerase chain reaction; DDM – N-dodecyl-β-D-maltoside; FTIR – Fourier-transform infrared

Abstract

Eukaryotic microbial rhodopsins are widespread bacteriorhodopsin-like proteins found in many lower eukaryotic groups including fungi. Many fungi contain multiple rhodopsins, some significantly diverged from the original bacteriorhodopsin template. Although few fungal rhodopsins have been studied biophysically, both fast-cycling light-driven proton pumps and slow-cycling photosensors have been found. The purpose of this study was to characterize photochemically a new subgroup of fungal rhodopsins, the so-called auxiliary group. The study used the two known rhodopsin genes from the fungal wheat pathogen, *Phaeosphaeria nodorum.* One of the genes is a member of the auxiliary group while the other is highly similar to previously characterized proton-pumping *Leptosphaeria* rhodopsin. Auxiliary rhodopsin genes from a range of species form a distinct group with a unique primary structure and are located in carotenoid biosynthesis gene cluster. Amino acid conservation pattern suggests that auxiliary rhodopsins retain the transmembrane core of bacteriorhodopsins, including all residues important for proton transport, but have unique polar intramembrane residues. Spectroscopic characterization of the two yeast-expressed *Phaeosphaeria* rhodopsins showed many similarities: absorption spectra, conformation of the retinal chromophore, fast photocycling, and carboxylic acid protonation changes. It is likely that both *Phaeosphaeria* rhodopsins are proton-pumping, at least *in vitro*. We suggest that auxiliary rhodopsins have separated from their ancestors fairly recently and have acquired the ability to interact with as yet unidentified transducers, performing a photosensory function without changing their spectral properties and basic photochemistry.

1. Introduction

Microbial rhodopsins are typical membrane proteins with seven transmembrane helical bundle similar to that of G-protein-coupled receptors [1-3]. Microbial rhodopsins are photosensitive, with all-*trans*-retinal as chromophore, covalently bound via the Schiff base to a Lys sidechain. Retinal photoisomerization triggers functionally important conformational changes in the protein (opsin) moiety. Since the last century, our perception of the functional, taxonomic, and ecological diversity of microbial rhodopsins has undergone a revolutionary change. Previously regarded as an eclectic mix of halobacterial light-driven proton and chloride pumps and related photosensory receptors, they have emerged as a large, widespread, multi-functional group found not only in *Archaea*, but in many *Bacteria* and *Eukarya*, including numerous fungal and algal species [2,4-7]. New functions were defined, including new types of photosensors, light-gated ion channels, and light-activated enzymes. We now recognise that many prokaryotic and eukaryotic species possess multiple rhodopsin (RD) and opsin-related protein (ORP) genes, which may have arisen both via gene duplication (often, multiple) and by lateral gene transfer [2,4].

There is clear evidence that fungal rhodopsins evolved via gene duplication and neofunctionalisation [6,8,9]. Fungal rhodopsins are clearly related to archaeal, rather than eubacterial, ancestors, most probably originating from the light-driven halobacterial proton pump, bacteriorhodopsin (BR) [2,10]. Some fungal opsins conserve the original haloarchael BR-like protein template and its proton pumping ability, whilst others lost the chromophore-binding lysine (these are not true opsins but opsin-related proteins (ORPs)), with a range of divergent forms in between [1,6,8]. The recent flood of genome sequences has shown that numerous fungal species possess multiple RDs and ORPs. However, few have been functionally characterised, and

their photobiological role is largely unknown.

The first identified homologs of BR in fungi were ORPs from yeast and basidiomycetes. On the basis that they were expressed during stress it was suggested they act as chaperones [11,12]. Their discovery was followed by the detection [13] and *in vitro* photochemical characterization [14] of *Neurospora crassa* rhodopsin (NR), which coexists with its ORP. Photochemical characterization of NR expressed in *Pichia pastoris* revealed a slow photocycle suggesting its role is photosensory rather than proton-pumping [14-16]. Phenotypic characterization of the knock-out mutants of NR (*nop*) (or its close homolog in *Fusarium fujikuroi* (*opsA*)) did not reveal an obvious function for NR, but implied participation in carotenoid biosynthesis regulation [17,18]. In contrast, the closely related rhodopsin from *Leptosphaeria maculans* (LR) [19] had a fast photocycle and could pump protons like BR [20,21]. Site-directed mutagenesis showed that one of the key differences responsible for the dramatically different photochemical behavior of NR and LR originated from a seemingly innocuous Asp/Glu replacement at the key position of the cytoplasmic proton donor to the retinal Schiff base [22,23]. Recent electrophysiological studies of NR (along with its close homolog in *Podospora anserina*) and LR expressed in neurons confirmed their drastically different proton-pumping abilities [24].

Thus, even the limited biochemical and physiological analysis available so far suggests multiple functions of fungal rhodopsins. Additionally, genomic information from several fungal species shows the existence of a third group of fungal rhodopsins; these have overall sequence resemblance to ORPs, but conserve all the key residues of the BR-like template [6,10]. We have tentatively called this group the auxiliary ORP-like rhodopsins, referring to their co-existence with other rhodopsin forms in the same species [10]. Auxiliary rhodopsins have been found in

many fungal species, but their expression pattern has been analyzed only in *Fusarium fujikuroi* [25] and *Bipolaris oryzae* [26] (plus distant homologs from basidiomycete *Ustilago maydis* [27]). A knock-out mutant of the *Fusarium fujikuroi* gene (*carO*) produced no phenotypical alterations under laboratory conditions. It may be linked to carotenoid metabolism as it is found in the carotenoid biosynthesis gene cluster [25,28]. So far, no auxiliary rhodopsin have been characterised physiologically or photochemically. Thus, one may only speculate about their role(s); a photosensory function tuned to a distinct spectral region is perhaps the most plausible hypothesis.

Here, we present photochemical characterization of an auxiliary rhodopsin using the protein from *Phaeosphaeria* (*Stagonospora*) *nodorum* (PhaeoRD2) and compare it with the LR-like homolog (PhaeoRD1) [29]. Both rhodopsins were expressed in *Pichia pastoris* and characterized spectroscopically. The two rhodopsins have similar absorption spectra, disproving the idea that the auxiliary species are needed to respond to light stimuli of different wavelengths. Spectroscopic and mutational data suggest that the auxiliary PhaeoRD2 may have some proton-pumping ability, similar to LR and PhaeoRD1.

2. Materials and Methods

2.1. Protein expression

Similar to our previous work on NR and LR [16,20,30], the two *Phaeosphaeria* rhodopsins were heterologously expressed in methylotrophic yeast (*Pichia pastoris*, strain GS115) with a yield of ~5 mg of purified protein per litre of culture. The *Phaeosphaeria* rhodopsin genes *Ops1* (SNOG_00807, Gene ID: 5968425, renamed PhaeoRD1) and *ops2* (SNOG_00341, Gene ID: 5967674, renamed PhaeoRD2) were cloned between the *EcoRI* and *XbaI* sites of the pPICZαA vector. The coding sequences were truncated (*ops1* to 795 bp and

ops2 to 822 bp) to remove most of the putative extramembrane parts of the N termini using sequence alignments with NR and LR. Such replacement of the native N-terminus with the yeast signal sequence produced robust expression and good membrane targeting in the past [14,20,30]. *EcoRI* site was created at the 5' ends of the rhodopsin genes, while *XbaI* site was at the 3' ends, and 6-His-tag coding sequence was added at the C-terminus by performing the polymerase chain reaction (PCR) with the following primers: PhaeoRD1 forward (5'GCGAATTCGAATCTGGCCAGAAGACCCTC3') and reverse (5'GCTCTAGATTAATGGTGATGGTGATGGTGCGCGCCGTCATCCTCACCGAG3'), and PhaeoRD2 forward (5'GCGAATTCGACCATGGCTCAGACTTG3') and reverse (5'GCTCTAGATTAATGGTGATGGTGATGGTGAACGTTGGCGGGGCCATCGAG3').

The pPICZαA-PhaeoRD1 and pPICZαA-PhaeoRD2 vectors were propagated in DH5α strain of *E. coli* in low salt LB medium with 25 μg/ml zeocin, isolated using Qiagen kit (QIAprep Spin Miniprep), and transformed into *P. pastoris* GS115 cells by electroporation according to the manual of the *Pichia* expression kit (Invitrogen). The transformed colonies were isolated from the YPDS/zeocin plates and screened for high expression levels of rhodopsins in small-scale cultures, similar to what was done with LR [20,23]. The cells were grown in 25 ml of BMGY medium in 250 ml baffled flasks, shaking at 30°C, 300 rpm for 1-2 days. As OD_{600} reached ~10, 2.5 ml of culture was centrifuged at 1,500g for 5 min at 4°C, resuspended in 25 ml of BMMY medium, and grown by shaking at 240 rpm, 30°C. After 24 h, additional 175 μl of 100% methanol (final concentration 0.7%) and 6.25 μl of 10 mM all-*trans*-retinal (isopropanol stock, final concentration 2.5 μM) were added into the culture. At different time points (24 h, 40 h, 48 h, and 52 h), 1 ml of the expression culture was taken and centrifuged at 1,500g for 5 min at 4°C. The expression level of the protein was evaluated by the intensity of the color of the yeast

pellet, and the colonies showing the most intense red color were selected for a large-scale expression.

The large-scale protein expression followed the established shake-flask protocol of the *Pichia* expression kit (Invitrogen) with small modifications. Briefly, a small amount of cells from a colony with the highest expression level of rhodopsins in small-scale cultures was inoculated into 25 ml of BMGY in a sterile 250 ml baffled flask. This seed culture was grown, shaking at 30°C (300 rpm) for 18–24 h, until the OD_{600} exceeded 2, and inoculated into a sterile 2 L baffled flask containing 250 ml of BMGY. This culture was shaken at 29–30°C (270 rpm) for 18–24 h, until the OD_{600} reached 3.6. To induce rhodopsin expression, the cells were pelleted in sterile containers at 1,500g for 5 min at 4°C, and gently resuspended in 0.8 L of BMMY, which was placed into 2.8 L Fernbach flask and shaken at 29–30°C (240 rpm). 10 mM isopropanol stock of all-*trans*-retinal (Sigma, final concentration 5 μM) and 100% filtered methanol (final concentration 0.7%) were added to the growth medium after 24 h of induction. The red-colored cells were collected by centrifugation at 1,500g for 5 min at 4°C after 40 h of induction, as the protein yield was found to be lower upon longer (48–52 h) and shorter (24 h) incubation times. The cell pellet was washed with MilliQ water twice and stored frozen at -20°C for later use.

D126N mutant of PhaeoRD2 was expressed analogously to the wild-type. To produce the mutant, two primers containing DNA for the desired mutation and high-fidelity thermostable Pwo polymerase were employed in a single-step PCR from the wild-type construct. To set up the polymerase chain reaction (PCR), 5’CCTTTGCTCCTGACCAACCTCATGCTCACCGC3’ and 5’GCGGTGAGCATGAGGTTGGTCAGGAGCAAAGG3’ primers were used.

2.2. Protein purification and lipid reconstitution

The cell breakage and protein purification protocols were based on those used for LR

[20,22,30] with small modifications. Cell pellets collected from the 800 ml of culture were re-suspended in one pellet volume of buffer A (7 mM NaH_2PO_4 at pH 6.5, 7 mM EDTA, 7 mM DTT, and 1 mM PMSF), incubated in the dark at room temperature for 3 h with 5 mg of lyticase (from *Arthrobacter luteus*, Sigma) for digestion of the cell walls, and additional 25 μM of all-*trans*-retinal to ensure complete rhodopsin regeneration. The cells were then centrifuged at 1,500g for 5 min at 4°C and resuspended in one pellet volume of buffer A. Half of the pellet volume of ice-cold acid-washed glass beads (Fisher) (420–600 μm diameter) was added, and the cells were disrupted with four 1 min pulses using vigorous vortexing. The cell debris were removed by centrifugation at 700g for 5 min at 4°C and the cell lysate was collected. An additional half pellet volume of buffer A was added to resuspend the cell debris, and vortexing and centrifugation steps were repeated several times to achieve complete breakage of the cells. All cell supernatants containing the membrane fraction were combined and centrifuged at 40,000g for 30 min (or at 150,000g for 50 min for smaller membrane fragments) at 4°C, and the membrane pellets were stored at -20°C for later use.

For visible spectroscopy experiments in the fungal membrane environment, the membrane pellets were washed with N-dodecyl-β-D-maltoside (DDM) to decrease the size of the membrane fragments and remove peripheral proteins and cell walls. The suspension was incubated at room temperature for 5 min and centrifuged at 5,000g for 5 min at 4°C. The maximal final DDM concentration in the mixture was 0.5%, as higher DDM concentrations solubilized the membranes fully. The colored supernatant was collected and centrifuged at 20,000g for 30 min at 4°C, the solubilized protein in the supernatant was discarded, and only the membrane-embedded proteins from the pellet were used to prepare rhodopsin-loaded polyacrylamide gels for spectroscopic measurements. The protein gels were equilibrated with the

desired buffer for at least 2 h before the measurements. As the D126N mutant of PhaeoRD2 was unstable after the DDM treatment, its photocycle (along with the wild-type controls) was measured in gels incorporating untreated yeast membranes.

To purify rhodopsins for reconstitution into liposomes needed for vibrational spectroscopy, we used 6-His tag affinity resin (Ni-NTA agarose, Qiagen). We estimated the quantity of solubilized proteins spectroscopically (Cary 50, Varian), assuming the molar extinction similar to that of BR. Due to different biochemical properties and stability of the two rhodopsins, the conditions for purification were different. To purify PhaeoRD1, the pellets of frozen membranes were resuspended with solubilization buffer (1% DDM, 20 mM KH_2PO_4, 1 mM PMSF, pH 7.5), and stirred in the dark at 4°C for 3-4 h, then centrifuged at 40,000g for 30 min at 4°C to remove unsolubilized material. The membrane pellets of PhaeoRD2 were resuspended in solubilization buffer (1% Triton X-100, 20 mM KH_2PO_4, 0.3 M NaCl, 10 mM β-mercaptoethanol, 1 mM PMSF, pH 7.5), and stirred in the dark at 4°C overnight, then centrifuged at 38,000 rpm for 50 min at 4°C. Solubilized rhodopsins were mixed with 6-His tag affinity resin and incubated in the dark at room temperature with gentle agitation to allow complete binding (usually 3 h). The clear supernatant containing other solubilized proteins was removed after centrifugation at 4,000g at 4°C for 2 min. The resin was washed with increasing concentrations of imidazole (0.25% DDM, 50 mM KH_2PO_4, 400 mM NaCl, up to 35 mM imidazole, pH 7.5 for PhaeoRD1, and 0.25% Triton-X100, 50mM KH_2PO_4, 400 mM NaCl, up to 35 mM imidazole, 1 mM DTT, pH 7.5 for PhaeoRD2) until the spectral cytochrome band at 410 nm disappeared from the wash spectrum. The purified proteins were eluted from the resin with the elution buffers of the same composition as the respective wash buffers, but with 250 mM imidazole. Addition of *Pichia* lipid extract (at 0.2 mg/ml) was needed to stabilize solubilized

PhaeoRD2, similar to what was found for NR [15].

The lipid reconstitution protocol followed that used for LR [30]. The dry powder lipids (DMPC: DMPA = 9:1 w/w, Avanti lipids) were first dissolved and mixed in warm chloroform, which was thoroughly removed by evaporation under vacuum to yield a thin lipid film. The dry lipids were rehydrated by 50 mM KH_2PO_4, 100 mM NaCl, pH 7.5 and agitated to obtain lipid suspension at high concentration (usually, 10 mg/ml). Purified solubilized rhodopsins were added to the preformed liposomes, which were semi-solubilized (as judged by the drop in turbidity) with Triton X-100 at protein/lipids/detergent (w/w/w) ratio of 1:3:1.5, and stirred for 15 min at room temperature. The resultant semi-transparent mixture became turbid after removal of detergent by adding 400 mg of Bio-beads SM-2 (Biorad) per 1 ml of the mixture and incubation with stirring at 4°C in the dark. The proteoliposomes were collected by centrifugation at 20,000g for 30 min at 4°C.

2.3. Visible and vibrational spectroscopy measurements

The static visible spectroscopy was performed with a Cary 50 spectrophotometer. The time-resolved visible spectra were collected using custom-built flash-photolysis equipment [20,31], with 7 ns excitation pulses of the second harmonic of a Nd-YAG laser at 532 nm (Continuum Minilite II). Light-induced absorption changes at different wavelengths were averaged (usually, several hundreds of traces) and converted into a quasilogarithmic time scale using in-house software.

Time-resolved difference FTIR spectra were gathered at 4 cm^{-1} resolution in a rapid-scan mode as described previously [20], using a Bruker IFS66vs apparatus with a temperature-controlled sample holder (Harrick) connected to a circulating water bath (Fisher). The photocyle was initiated by the laser pulses as described above. The films of hydrated DMPA:DMPC

liposomes were compressed between two CaF_2 windows with 6 μm spacer, and data acquisition was controlled by the OPUS software (Bruker). Static Raman spectra were collected using FRA106/s accessory to the IFS66vs spectrometer, with excitation at 1024 nm, at 2 cm^{-1} resolution.

3. Results and Discussion

3.1. Sequence-based Analysis

The *Phaeosphaeria nodorum* genome annotation [29] included two rhodopsins. Ops 1 (or PhaeoRD1) is very similar to LR, while the second rhodopsin (PhaeoRD2) belongs to a new subgroup, not characterized spectroscopically [10]. We called this subgroup "auxiliary", because most of its members were found in addition to other rhodopsin forms. Since then, many new fungal genomes have become publicly available, so that the placement of *Phaeosphaeria* rhodopsins, as well as clustering of fungal rhodopsins in general, can be reevaluated with much greater confidence. Thus, we first compared amino acid sequences of the two *Phaeosphaeria* opsins to the sequences of opsins (full sequences only, excluding ORPs) from other ascomycetes, using publicly available genome databases (http://blast.ncbi.nlm.nih.gov/; http://genome.jgi-psf.org/; http://www.broadinstitute.org/).

The results of CLUSTALW analysis confirm our earlier suggestion [10] that auxiliary rhodopsins form a very distinct branch on the fungal rhodopsin tree (boxed in Fig. 1). The analyzed fungal rhodopsins can be divided into two large subgroups. Within each of the subgroups, the rhodopsins align with species phylogenies [32]. The first subgroup includes previously characterized putative photosensors and proton pumps such as NR and LR. Many of the fungal species found in this first group, especially those from *Pleosporomycetidae*,

Dothideomycetidae, *Helotiales*, and *Hypocreomycetidae*, have additional, second rhodopsin forms in the second (auxiliary) subgroup. Additionally, the auxiliary subgroup contains third and fourth forms of rhodopsins of *Dothideomycetidae* and a few standalone (if we disregard ORPs) rhodopsins, e.g., from several species of *Colletotrichum* and *Verticillium* (Fig. 1). It is clear that, as suggested before, PhaeoRD1 is the closest homolog of LR (79% identity, 91% similarity), and as such belongs to the first subgroup, while PhaeoRD2 is a member of the auxiliary cluster, with distinct amino acid sequence (35% identity, 53% similarity to LR). This analysis suggested that the photochemical and functional properties of PhaeoRD1 would be LR-like, while those of PhaeoRD2 were unknown.

In view of the earlier finding that the auxiliary rhodopsin from *Gibberella* (*Fusarium*) *fujikuroi*, *carO*, was found in a carotenoid biosynthesis cluster that also contains a carotene oxygenase *carX*, phytoene synthase/cyclase *carRA* and phytoene desaturase *carB* [25], we explored the genomic context for the members of this group. The cluster structure is preserved in *Helotiales* (*Botrytis* and *Sclerotinia*) and *Hypocreomycetidae* (*Gibberella zeae, Gibberella moniliformis, Fusarium oxysporum, Nectria*), and selected *Dothideomycetes* (*Mycosphaerella graminicola* and *Rhytidhysteron rufulum*). In the *Pleosporomycetidae* (*Phaeosphaeria*, *Leptosphaeria*, *Pyrenophora*, *Alternaria*, *Cochliobolus, Setosphaeria*) gene orders and orientations are shuffled (as seen in many fungal gene clusters, e.g. [29]), in a local reflection of mesosynteny [33]. The clustering of auxiliary rhodopsins with carotenoid biosynthesis genes is strongly suggestive of a carotenoid-related physiological role and expression regulation as described for *carO* [18,28].

To gain further insight into the structural differences between the two major rhodopsin subgroups, we have aligned amino acid sequences of the representative members of the auxiliary

subgroup (restricted to second rhodopsin forms, including PhaeoRD2) (Fig. 2) and compared the conservation pattern in the last six transmembrane helices (most conserved in microbial rhodopsins) with that known for BR and LR [10,19,34]. The full-length alignment (except for the non-conserved termini) of a broader selection of sequences is available in the supplementary data file. The first general trend observed from the alignment is a very high degree of conservation of the BR-like template (shown yellow on black) in fungal rhodopsins of both subgroups. The conserved residues include most of the retinal-binding pocket and the majority of amino acids implicated in the light-driven proton transport (BR's T46, Y57, R82, D85, T89, T90, D96, D115, W182, Y185, W189, E194, E204, D212, and many others). This suggests that auxiliary rhodopsins may possess proton pumping ability similar to that observed for LR [20], as they conserve all major proton donors and acceptors of BR. It must be noted that the primary proton donor (homolog of BR's D96) is strictly conserved as Asp in the auxiliary subgroup, as it is known that its conservative replacement by Glu can strongly impede the proton transport in NR and mutant LR [22]. From the conservation pattern of the BR template in fungi, it is impossible to reliably predict which one of the subgroups is evolutionary closer to the archaeal ancestor, as there is almost equal number of cases of exclusive conservation of BR residues in each subgroup. On the other hand, our CLUSTALW analysis of the full-length opsin sequences (not shown) places BR somewhat closer to the first subgroup, in agreement with the previous analysis [18].

Next, we analyzed distribution of the residues uniquely conserved in the auxiliary subgroup (highlighted purple in Fig. 2) relative to the putative membrane core of these proteins, as defined by homology to BR structure. While most of the unique residues are located at the ends of the helices in the membrane interfacial regions, there are notable exceptions, the most striking of which is helix D. Even though there are several uniquely conserved residues in the

middle of the helices E and F, they do not change the overall character of those helices, being mere changes in size of the affected hydrophobic sidechains. On the contrary, there must be a dramatic change in the properties of the helix D, as a result of the introduction of a polar residue with hydrogen bonding ability into the middle of the transmembrane domain, corresponding to position 116 of BR, along with a number of other changes (Fig. 2). The polar residue in the middle of helix D of fungal rhodopsins from the auxiliary group is usually represented by Glu, and sometimes by Trp, and follows the super-conserved homolog of Asp-115 of BR. This puts severe constraints on the possible sidechain orientation of this new polar residue. As Asp-115 is hydrogen-bonded to Thr-90 from helix C in BR, and this pair is preserved in all fungal rhodopsins, one may expect that the following Glu-116 will face the core of the lipid bilayer. This is highly unlikely, unless it is used to interact with a protein partner (either an unknown transducer or another rhodopsin molecule, leading to oligomerization). From this tentative analysis, one may speculate that rhodopsins of the auxiliary subgroup have preserved their proton-pumping ability, but have also acquired capacity to interact with membrane-bound transducers. This is reminiscent of the evolutionary relationship between BR and halobacterial sensory rhodopsins, which preserved rudimentary proton-pumping ability in the absence of their transducers and use the same conformational changes as proton pumps to perform signaling [35,36].

3.2. Photochemical Characterization

Both *Phaeosphaeria* opsins expressed in *Pichia pastoris* formed red pigments upon addition of all-*trans*-retinal, which were stable both in the yeast membranes and upon reconstitution of the purified proteins into synthetic lipids. The dark states of the obtained

chromoproteins were first characterized by the visible and Raman spectroscopies (Fig. 3). The maxima of the visible absorption spectra of both proteins were similar and close to that observed for LR (542 nm in yeast membranes [20]). Purified solubilized proteins have absorption maxima at 540 nm for PhaeoRD1 and 535 nm for Phaeo RD2 (Fig. 3, left panel), and the respective maxima are at 545 nm and 538 nm in yeast membranes (not shown). No apparent light- or dark-adaptation was observed, similar to the case of LR [20,21]. According to the Raman spectroscopy results (Fig. 3, right panel), which report mostly on the retinal chromophore, the dark states contain predominantly all-*trans*-retinal. This is obvious from the prominent pair of C-C stretching vibrations around 1202 and 1168 cm^{-1}, similar to those of light-adapted BR and LR [20,37]. The location of the major ethylenic C=C stretches (at 1533 cm^{-1} for PhaeoRD1 and at 1537 cm^{-1} for PhaeoRD2) is consistent with their visible maxima, where higher frequency correlates with more blue-shifted visible absorption [38]. From the characterization of the dark states, we can conclude that it is unlikely that these two rhodopsin forms exist solely to respond to different wavelength of visible light, as their absorption maxima are very close to each other and both fall into the green region. It can be also argued that the retinal-binding pockets of both *Phaeosphaeria* opsins must be similar to that of LR, which is expected from the conservation of their transmembrane regions (Fig. 2), as they show very close visible maxima and similar vibrational spectra of the chromophore.

Next, we characterized the photochemical cycles of both *Phaeosphaeria* rhodopsins using time-resolved spectroscopy in the visible range. As expected from the high degree of sequence identity of PhaeoRD1 and LR, their photochemistry was very similar (Fig. 4, lower panel). At neutral pH, the photocycle of PhaeoRD1 is quite fast, finishing in a few tens of milliseconds, as expected for proton pumps [1,10]. It has a well-defined M intermediate with the

deprotonated retinal Schiff base (observed at 400 nm), which forms on a submillisecond time scale and decays in a pH-dependent manner (Fig. 4, upper panel), again, similar to LR [20], but with somewhat stronger pH-dependence (see below). At lower pH, the reprotonation of the Schiff base (M decay) is fast (a few ms), and the M intermediate is followed by a red-shifted intermediate, which disappears at higher pH, when the M decay becomes slow. The only notable difference in the photocycle kinetics of PhaeoRD1 and LR is a higher accumulation of the early red-shifted intermediate along with the early M intermediate on the tens of microseconds time scale, which may point at a somewhat shifted protonation equlibrium between the Schiff base and the primary proton acceptor. From the early parts of the 460 nm kinetics, it is also obvious that an L-like intermediate accumulates in equilibrium with the K-like and the early M states. But this difference does not affect the later parts of the photocycle of PhaeoRD1, which is consistent with the expected LR-like photochemistry of a light-driven proton pump.

The photocycle kinetics of PhaeoRD2, on the contrary, appears to be quite different from those of PhaeoRD1 and LR (Fig. 5). On the one hand, the overall kinetics of the photocycle is quite fast, with the turnover characteristic time of a few tens of ms at neutral pH, which is consistent with a proton-pumping rhodopsin behavior, similar to PhaeoRD1. On the other hand, kinetics of the rise and decay, as well as relative concentrations of photointermediates, differ dramatically for the two *Phaeosphaeria* rhodopsins (Fig. 5, lower panel). The most striking feature of the photocycle of PhaeoRD2 is an extremely fast deprotonation of the retinal Schiff base, as observed by the rise of the M intermediate at 400 nm. The plateau of the M intermediate concentration is reached in less than 10 microseconds, as opposed to the sub-millisecond plateau in PhaeoRD1, LR, and BR. Such extremely fast pH-independent deprotonation of the retinal Schiff base is typical for BR mutants with perturbed protonation equilibria between the Schiff

base nitrogen and Asp-85, especially as found in mutants involving Arg-82 [39]. While homologs of Arg-82, as well as of other important members of the extracellular hydrogen-bonded network (Tyr-57, Glu-194, Glu-204) [40], are conserved in all auxiliary fungal rhodopsins, there are many unique residues in the extracellular loops and interfacial regions (Fig. 2 and supplementary file). These unique residues could interact with the sidechain of the homolog of Arg-82 in PhaeoRD2 and change its position, affecting the pKa of the primary proton acceptor (homolog of Asp-85) via the well-described coupling mechanism [41-43]. Additionally, even though the kinetics of the Schiff base reprotonation (the M decay at 400 nm) are similarly fast and pH-dependent for PhaeoRD1 and PhaeoRD2, the accumulation of the late red-shifted intermediate (observed at 620 nm) is much higher in PhaeoRD1, possibly due to its faster decay in PhaeoRD2. It should be noted that the pH-dependence of the Schiff base reprotonation in both proteins (Fig. S1) is much more strongly pH-dependent than that in BR (and even LR). The persistence of the fast phase of the Schiff base reprotonation in BR is usually explained by the internal nature of its proton donor, Asp-96. The absence of such phenomenon can be interpreted as a sign of a lower pK_a of its homologs in the N-like intermediates in *Phaeosphaeria* rhodopsins.

The fast reprotonation of the Schiff base along with the rapid photocycle turnover in PhaeoRD2 hints at the possibility that it may have some proton-pumping ability. This would be consistent with the sequence analysis presented above, which showed the presence of the conserved homolog of Asp-96 of BR, Asp-126, possibly serving as an internal cytoplasmic proton donor to the Schiff base, ensuring its fast reprotonation. To verify that idea, we replaced the putative cytoplasmic proton donor Asp-126 with non-protonatable Asn and studied the photocyle of the D126N mutant (Fig. 6). If Asp-126 is indeed the primary proton donor for the Schiff base of PhaeoRD2, one would expect a dramatically slower Schiff base reprotonation (M

decay at 400 nm), similar to what was observed for LR [20,22]. Consistent with these expectations, we observed extremely slow (on the seconds time scale) pH-dependent M decay (Fig. 6, upper panel, and Fig. S1). While such dramatic deceleration of the Schiff base reprotonation is indicative of the proton-donating role of the replaced Asp-126, there is a possibility that it may occur through the global conformational effect of the D126N mutation. The latter hypothesis can be easily disproved by checking the effect of a common artificial proton shuttle, sodium azide (NaN_3), which is known to accelerate the Schiff base reprotonation in the homologous mutants of microbial rhodopsins [20,44]. Addition of 1 mM NaN_3 (Fig. 6, lower panel) restored the wild-type-like kinetics of the Schiff base reprotonation (millisecond time scale), confirming the proton-donating role of Asp-126.

Taken together, the photocycle kinetics data obtained by visible spectroscopy on the wild-type and mutant PhaeoRD2 strongly argue for its proton-pumping ability, even though we could not verify it directly, due to the instability of PhaeoRD2 under continuous illumination in liposomes. At the same time, it is conceivable that the photocycle of PhaeoRD2 (as well as its proton-pumping ability) are different *in vivo*, upon interaction with its putative transducer (in the case it is a photosensory rhodopsin as hinted by the sequence analysis). As dramatic changes in the photochemistry and ion transport are known for halobacterial sensory rhodopsins [45-47], *in vitro* kinetic data should be treated with caution.

To obtain further insight into the molecular details of light-induced proton transfers and conformational changes of the retinal chromophore and the opsin moiety of the *Phaeosphaeria* rhodopsins, we employed time-resolved difference Fourier-transform infrared (FTIR) spectroscopy. Figure 7 compares difference FTIR spectra of PhaeoRD1 and PhaeoRD2 taken at a few ms after the excitation. From the results of the visible spectroscopy, both spectra were

expected to be dominated by the M intermediate, with some contribution from a later red-shifted intermediate in the case of PhaeoRD1. This is indeed the case, as can be observed from the C-C stretching vibrations region (fingerprints), which shows only negative bands [48,49] corresponding to all-*trans*-retinal of the dark state for PhaeoRD2 (1201 and 1168 cm^{-1}, lower panel), with a weak positive band of 13-*cis*-retinal of a late photointermediate at 1188 cm^{-1} for PhaeoRD1 (upper panel). The latter band becomes prominent in the PhaeoRD1 spectra taken at 25 ms delay after the flash (Fig. S2), consistent with the expected rise of the late intermediate and decay of M. Overall, the FTIR difference spectra of PhaeoRD1 corresponding to the M intermediate (Fig. 7, upper panel), as well as to the late intermediate (not shown), are very similar to the corresponding spectra of LR [20]. Among the most typical and important opsin bands observed both for PhaeoRD1 and LR, one should mention those of protonation of the primary proton acceptor (homolog of D85 of BR) at 1759 cm^{-1}, and the perturbation of the homolog of BR's D115 at 1741/1736 cm^{-1}. At a later delay (25 ms, Fig. S2), an additional negative band assigned to the deprotonation of the homolog of the primary proton donor D96 was observed at 1745 cm^{-1}. Additionally, prominent bands at 1390/1381 cm^{-1} recently assigned to deprotonated carboxylic acids in isotope-labeled LR [30] were observed in PhaeoRD1 as well. Most retinal bands were identical or very similar between LR and PhaeoRD1, consistent with the Raman data (Fig. 3), including C=C stretches at 1533 cm^{-1}, C-C stretches (with other contributions) at 1250, 1201, 1169 cm^{-1}, and putative Schiff base vibrations at 1643/1620 cm^{-1}.

Surprisingly, the FTIR difference spectra of PhaeoRD2, dominated by the M intermediate (Fig. 7, lower panel) were very similar to those obtained for PhaeoRD1 and LR. Some minor differences in the FTIR spectra of *Phaeosphaeria* rhodopsins originate from the different mixtures of intermediates (almost pure M for PhaeoRD2 and mixture of M with a later

intermediate in PhaeoRD1). It should be noted, that at higher pH, the appearance of an N-like signatures of 13-*cis*-retinal and deprotonated homolog of Asp-96 of BR can be observed (Fig. S2), similar to those in PhaeoRD1 at longer delay times. Overall, in spite of the differences in the photocycle kinetics and the amino acid sequences, all the major vibrational bands of retinal and carboxylic acids discussed above for PhaeoRD1 were observed for PhaeoRD2 as well. This points to the high degree of conservation of the transmembrane core of BR in the auxiliary rhodopsin group and that the light-induced isomerization of retinal and ensuing proton transfers are very similar for the LR-like PhaeoRD1 and auxiliary PhaeoRD2. There are a number of differences between the two rhodopsins in several opsin bands in the range of Amide I and Asn/Gln sidechain vibrations (1700-1600 cm^{-1}), which may reflect the differences in the conformational changes of the proteins' interfacial regions expected from the differences in the primary structures, but at this point we can not assign them.

3.3. Conclusions

We studied a new subgroup of fungal rhodopsins (termed the auxiliary group [10]), using sequence analysis of the fungal genomic data and photochemical comparison of two representative rhodopsins from *Phaeosphaeria nodorum* [29]. The bioinformatic analysis confirms that the auxiliary subgroup forms a very distinct cluster on the rhodopsin tree (Fig. 1) due to the unique primary structure of its members (Fig. 2), which are usually present in addition to other rhodopsin forms in their host species. Evidently, the auxiliary group diverged from the other rhodopsisn early in the history of the ascomyota, some 400 Mya [50]. Analysis of the genomic context shows that auxiliary rhodopsins may be linked to the carotenoid biosynthesis cluster of genes. Structural analysis of the conserved regions suggests that auxiliary rhodopsins

preserved the common transmembrane core of BR and LR, but have some polar residues on the hydrophobic protein periphery, which may suggest interactions with a putative transducer or other membrane partner.

Spectroscopic analysis by the visible, Raman, and FTIR spectroscopy reveals some characteristic photocycle features for the auxiliary rhodopsin of *Phaeosphaeria*, but also confirms conservation of the main BR-like characteristics. Close similarity of the absorption spectra of the two *Phaeosphaeria* rhodopsins (LR-like and auxiliary) implies that they are not designed to interact with different wavelengths of light. The photocycles of both rhodopsins are fast, and show photointermediates and proton transfer steps typical for proton-pumping rhodopsins. Taken together with the distinct phenotype of the auxiliary rhodopsin in which the cytoplasmic Schiff base proton donor is disabled, it suggests that auxiliary rhodopsins preserved their proton-pumping ability, at least in the absence of their putative transducers. We suggest that this may point to a fairly recent evolutionary separation of these putative photosensors. Whether the auxiliary rhodopsins indeed serve as photosensors remains to be seen by the future *in vivo* experiments.

Acknowledgements

The research was supported by grants from the Canada Foundation for Innovation/Ontario Innovation Trust, the Natural Sciences and Engineering Research Council of Canada (NSERC), the Research Corporation (Tucson, AZ), and the University of Guelph to L.S.B. Y.F. is a recipient of the NSERC doctoral scholarship.

References

[1] J.L. Spudich, C.S. Yang, K.H. Jung, E.N. Spudich, Retinylidene proteins: Structures and functions from archaea to humans, Annual Review of Cell and Developmental Biology, 16 (2000) 365-392.

[2] A.K. Sharma, J.L. Spudich, W.F. Doolittle, Microbial rhodopsins: functional versatility and genetic mobility, Trends in Microbiology, 14 (2006) 463-469.

[3] J.P. Klare, I. Chizhov, M. Engelhard, Microbial rhodopsins: scaffolds for ion pumps, channels, and sensors, Results Probl Cell Differ, 45 (2008) 73-122.

[4] M.X. Ruiz-Gonzalez, I. Marin, New insights into the evolutionary history of type 1 rhodopsins, J Mol Evol, 58 (2004) 348-358.

[5] P. Hegemann, Algal sensory photoreceptors, Annu Rev Plant Biol, 59 (2008) 167-189.

[6] L.S. Brown, Fungal rhodopsins and opsin-related proteins: eukaryotic homologues of bacteriorhodopsin with unknown functions, Photochemical & Photobiological Sciences, 3 (2004) 555-565.

[7] J.L. Spudich, The multitalented microbial sensory rhodopsins, Trends Microbiol, 14 (2006) 480-487.

[8] A. Idnurm, S. Verma, L.M. Corrochano, A glimpse into the basis of vision in the kingdom Mycota, Fungal Genet Biol, 47 (2010) 881-892.

[9] J. Rodriguez-Romero, M. Hedtke, C. Kastner, S. Muller, R. Fischer, Fungi, hidden in soil or up in the air: light makes a difference, Annu Rev Microbiol, 64 (2010) 585-610.

[10] L.S. Brown, K.H. Jung, Bacteriorhodopsin-like proteins of eubacteria and fungi: the extent of conservation of the haloarchaeal proton-pumping mechanism, Photochemical & Photobiological Sciences, 5 (2006) 538-546.

[11] R.C. Graul, W. Sadee, Evolutionary relationships among proteins probed by an iterative neighborhood cluster analysis (INCA). Alignment of bacteriorhodopsins with the yeast sequence YRO2, Pharm Res, 14 (1997) 1533-1541.

[12] Y. Zhai, W.H. Heijne, D.W. Smith, M.H. Saier, Jr., Homologues of archaeal rhodopsins in plants, animals and fungi: structural and functional predications for a putative fungal chaperone protein, Biochim Biophys Acta, 1511 (2001) 206-223.

[13] J.A. Bieszke, E.L. Braun, L.E. Bean, S. Kang, D.O. Natvig, K.A. Borkovich, The nop-1 gene of Neurospora crassa encodes a seven transmembrane helix retinal-binding protein homologous to archaeal rhodopsins, Proc Natl Acad Sci U S A, 96 (1999) 8034-8039.

[14] J.A. Bieszke, E.N. Spudich, K.L. Scott, K.A. Borkovich, J.L. Spudich, A eukaryotic protein, NOP-1, binds retinal to form an archaeal rhodopsin-like photochemically reactive pigment, Biochemistry-Us, 38 (1999) 14138-14145.

[15] L.S. Brown, A.K. Dioumaev, J.K. Lanyi, E.N. Spudich, J.L. Spudich, Photochemical reaction cycle and proton transfers in neurospora rhodopsin, J Biol Chem, 276 (2001) 32495-32505.

[16] Y. Furutani, A.G. Bezerra, S.A. Waschuk, M. Sumii, L.S. Brown, H. Kandori, FTIR spectroscopy of the K photointermediate of Neurospora rhodopsin: structural changes of the retinal, protein, and water molecules after photoisomerization., Biochemistry-Us, 43 (2004) 9636-9646.

[17] J.A. Bieszke, L. Li, K.A. Borkovich, The fungal opsin gene nop-1 is negatively-regulated by a component of the blue light sensing pathway and influences conidiation-specific gene expression in Neurospora crassa, Curr Genet, 52 (2007) 149-157.

[18] A.F. Estrada, J. Avalos, Regulation and targeted mutation of opsA, coding for the NOP-1 opsin orthologue in Fusarium fujikuroi, J Mol Biol, 387 (2009) 59-73.

[19] A. Idnurm, B.J. Howlett, Characterization of an opsin gene from the ascomycete Leptosphaeria maculans, Genome, 44 (2001) 167-171.

[20] S.A. Waschuk, A.G. Bezerra, L. Shi, L.S. Brown, Leptosphaeria rhodopsin: Bacteriorhodopsin-like proton pump from a eukaryote, P Natl Acad Sci USA, 102 (2005) 6879-6883.

[21] M. Sumii, Y. Furutani, S.A. Waschuk, L.S. Brown, H. Kandori, Strongly hydrogen-bonded water molecule present near the retinal chromophore of Leptosphaeria rhodopsin, the bacteriorhodopsin-like proton pump from a eukaryote, Biochemistry-Us, 44 (2005) 15159-15166.

[22] Y. Furutani, M. Sumii, Y. Fan, L.C. Shi, S.A. Waschuk, L.S. Brown, H. Kandori, Conformational coupling between the cytoplasmic carboxylic acid and the retinal in a fungal light-driven proton pump, Biochemistry-Us, 45 (2006) 15349-15358.

[23] Y. Fan, L. Shi, L.S. Brown, Structural basis of diversification of fungal retinal proteins probed by site-directed mutagenesis of Leptosphaeria rhodopsin, Febs Lett, 581 (2007) 2557-2561.

[24] B.Y. Chow, X. Han, A.S. Dobry, X. Qian, A.S. Chuong, M. Li, M.A. Henninger, G.M. Belfort, Y. Lin, P.E. Monahan, E.S. Boyden, High-performance genetically targetable optical neural silencing by light-driven proton pumps, Nature, 463 (2010) 98-102.
[25] M.M. Prado, A. Prado-Cabrero, R. Fernandez-Martin, J. Avalos, A gene of the opsin family in the carotenoid gene cluster of Fusarium fujikuroi, Curr Genet, 46 (2004) 47-58.
[26] J. Kihara, N. Tanaka, M. Ueno, S. Arase, Cloning and expression analysis of two opsin-like genes in the phytopathogenic fungus Bipolaris oryzae, FEMS Microbiol Lett, 295 (2009) 289-294.
[27] A.F. Estrada, T. Brefort, C. Mengel, V. Diaz-Sanchez, A. Alder, S. Al-Babili, J. Avalos, Ustilago maydis accumulates beta-carotene at levels determined by a retinal-forming carotenoid oxygenase, Fungal Genet Biol, 46 (2009) 803-813.
[28] J. Avalos, A.F. Estrada, Regulation by light in Fusarium, Fungal Genet Biol, 47 (2010) 930-938.
[29] J.K. Hane, R.G. Lowe, P.S. Solomon, K.C. Tan, C.L. Schoch, J.W. Spatafora, P.W. Crous, C. Kodira, B.W. Birren, J.E. Galagan, S.F. Torriani, B.A. McDonald, R.P. Oliver, Dothideomycete plant interactions illuminated by genome sequencing and EST analysis of the wheat pathogen Stagonospora nodorum, Plant Cell, 19 (2007) 3347-3368.
[30] Y. Fan, L. Shi, V. Ladizhansky, L.S. Brown, Uniform isotope labeling of a eukaryotic seven-transmembrane helical protein in yeast enables high-resolution solid-state NMR studies in the lipid environment, J Biomol Nmr, 49 (2011) 151-161.
[31] L.C. Shi, S.R. Yoon, A.G. Bezerra, K.H. Jung, L.S. Brown, Cytoplasmic shuttling of protons in Anabaena sensory rhodopsin: Implications for signaling mechanism, J Mol Biol, 358 (2006) 686-700.
[32] C.L. Schoch, G.H. Sung, F. Lopez-Giraldez, J.P. Townsend, J. Miadlikowska, V. Hofstetter, B. Robbertse, P.B. Matheny, F. Kauff, Z. Wang, C. Gueidan, R.M. Andrie, K. Trippe, L.M. Ciufetti, A. Wynns, E. Fraker, B.P. Hodkinson, G. Bonito, J.Z. Groenewald, M. Arzanlou, G.S. de Hoog, P.W. Crous, D. Hewitt, D.H. Pfister, K. Peterson, M. Gryzenhout, M.J. Wingfield, A. Aptroot, S.O. Suh, M. Blackwell, D.M. Hillis, G.W. Griffith, L.A. Castlebury, A.Y. Rossman, H.T. Lumbsch, R. Lucking, B. Budel, A. Rauhut, P. Diederich, D. Ertz, D.M. Geiser, K. Hosaka, P. Inderbitzin, J. Kohlmeyer, B. Volkmann-Kohlmeyer, L. Mostert, K. O'Donnell, H. Sipman, J.D. Rogers, R.A. Shoemaker, J. Sugiyama, R.C. Summerbell, W. Untereiner, P.R. Johnston, S. Stenroos, A. Zuccaro, P.S. Dyer, P.D. Crittenden, M.S. Cole, K. Hansen, J.M. Trappe, R. Yahr, F. Lutzoni, J.W. Spatafora, The Ascomycota tree of life: a phylum-wide phylogeny clarifies the origin and evolution of fundamental reproductive and ecological traits, Syst Biol, 58 (2009) 224-239.
[33] J.K. Hane, T. Rouxel, B.J. Howlett, G.H.J. Kema, S.B. Goodwin, R.P. Oliver, A novel mode of chromosomal evolution peculiar to filamentous Ascomycete fungi, Genome Biol, (2011) in press.
[34] K. Ihara, T. Umemura, I. Katagiri, T. Kitajima-Ihara, Y. Sugiyama, Y. Kimura, Y. Mukohata, Evolution of the archaeal rhodopsins: evolution rate changes by gene duplication and functional differentiation, J Mol Biol, 285 (1999) 163-174.
[35] Y. Sudo, J.L. Spudich, Three strategically placed hydrogen-bonding residues convert a proton pump into a sensory receptor, P Natl Acad Sci USA, 103 (2006) 16129-16134.
[36] J.P. Klare, E. Bordignon, M. Engelhard, H.J. Steinhoff, Sensory rhodopsin II and bacteriorhodopsin: Light activated helix F movement, Photochemical & Photobiological Sciences, 3 (2004) 543-547.
[37] S.O. Smith, M.S. Braiman, A.B. Myers, J.A. Pardoen, J.M.L. Courtin, C. Winkel, J. Lugtenburg, R.A. Mathies, Vibrational Analysis of the All-Trans-Retinal Chromophore in Light-Adapted Bacteriorhodopsin, J Am Chem Soc, 109 (1987) 3108-3125.
[38] H. Kakitani, T. Kakitani, H. Rodman, B. Honig, R. Callender, Correlation of Vibrational Frequencies with Absorption Maxima in Polyenes, Rhodopsin, Bacteriorhodopsin, and Retinal Analogs, J Phys Chem-Us, 87 (1983) 3620-3628.
[39] S.P. Balashov, R. Govindjee, M. Kono, E. Imasheva, E. Lukashev, T.G. Ebrey, R.K. Crouch, D.R. Menick, Y. Feng, Effect of the arginine-82 to alanine mutation in bacteriorhodopsin on dark adaptation, proton release, and the photochemical cycle, Biochemistry-Us, 32 (1993) 10331-10343.
[40] H. Luecke, B. Schobert, H.T. Richter, J.P. Cartailler, J.K. Lanyi, Structure of bacteriorhodopsin at 1.55 angstrom resolution, J Mol Biol, 291 (1999) 899-911.
[41] H.T. Richter, L.S. Brown, R. Needleman, J.K. Lanyi, A linkage of the pK(a)'s of asp-85 and glu-204 forms part of the reprotonation switch of bacteriorhodopsin, Biochemistry-Us, 35 (1996) 4054-4062.
[42] H. Luecke, B. Schobert, J.P. Cartailler, H.T. Richter, A. Rosengarth, R. Needleman, J.K. Lanyi, Coupling photoisomerization of retinal to directional transport in bacteriorhodopsin, J Mol Biol, 300 (2000) 1237-1255.
[43] S.P. Balashov, R. Govindjee, E.S. Imasheva, S. Misra, T.G. Ebrey, Y. Feng, R.K. Crouch, D.R. Menick, The two pKa's of aspartate-85 and control of thermal isomerization and proton release in the arginine-82 to

lysine mutant of bacteriorhodopsin, Biochemistry-Us, 34 (1995) 8820-8834.
[44] J. Tittor, C. Soell, D. Oesterhelt, H.J. Butt, E. Bamberg, A defective proton pump, point-mutated bacteriorhodopsin Asp96----Asn is fully reactivated by azide, The EMBO journal, 8 (1989) 3477-3482.
[45] J. Sasaki, J.L. Spudich, Proton transport by sensory rhodopsins and its modulation by transducer-binding, Biochim Biophys Acta, 1460 (2000) 230-239.
[46] Y. Sudo, M. Iwamoto, K. Shimono, M. Sumi, N. Kamo, Photo-induced proton transport of pharaonis phoborhodopsin (sensory rhodopsin II) is ceased by association with the transducer, Biophys J, 80 (2001) 916-922.
[47] G. Schmies, M. Engelhard, P.G. Wood, G. Nagel, E. Bamberg, Electrophysiological characterization of specific interactions between bacterial sensory rhodopsins and their transducers, P Natl Acad Sci USA, 98 (2001) 1555-1559.
[48] C. Zscherp, J. Heberle, Infrared difference spectra of the intermediates L, M, N, and O of the bacteriorhodopsin photoreaction obtained by time-resolved attenuated total reflection spectroscopy, J Phys Chem B, 101 (1997) 10542-10547.
[49] W.G. Chen, M.S. Braiman, Kinetic-Analysis of Time-Resolved Infrared Difference Spectra of the L-Intermediates and M-Intermediates of Bacteriorhodopsin, Photochemistry and Photobiology, 54 (1991) 905-910.
[50] T. Rouxel, J. Grandaubert, J.K. Hane, C. Hoede, A.P. van de Wouw, A. Couloux, V. Dominguez, V. Anthouard, P. Bally, S. Bourras, A.J. Cozijnsen, L.M. Ciuffetti, A. Degrave, A. Dilmaghani, L. Duret, I. Fudal, S.B. Goodwin, L. Gout, N. Glaser, J. Linglin, G.H. Kema, N. Lapalu, C.B. Lawrence, K. May, M. Meyer, B. Ollivier, J. Poulain, C.L. Schoch, A. Simon, J.W. Spatafora, A. Stachowiak, B.G. Turgeon, B.M. Tyler, D. Vincent, J. Weissenbach, J. Amselem, H. Quesneville, R.P. Oliver, P. Wincker, M.H. Balesdent, B.J. Howlett, Effector diversification within compartments of the Leptosphaeria maculans genome affected by Repeat-Induced Point mutations, Nat Commun, 2 (2011) 202.
[51] J.D. Thompson, T.J. Gibson, D.G. Higgins, Multiple sequence alignment using ClustalW and ClustalX, Curr Protoc Bioinformatics, Chapter 2 (2002) Unit 2 3.
[52] R.D. Page, TreeView: an application to display phylogenetic trees on personal computers, Comput Appl Biosci, 12 (1996) 357-358.

Figure Legends

Figure 1. *Phaeosphaeria* rhodopsins as representatives of the two major subgroups of fungal rhodopsins. Unrooted guide tree of fungal rhodopsin sequences from ascomycetes (excluding OPRs) produced from the CLUSTALW [51] alignment and plotted using TREEVIEW [52]. Numbers after the names of fungal species indicate multiple forms of rhodopsins found in the same species. The scale bar represents number of substitutions per site (0.1 indicates 10 nucleotide substitutions per 100 nucleotides). *Phaeosphaeria* rhodopsins studied in this work are highlighted yellow, previously characterized rhodopsins are highlighted purple, and the auxiliary subgroup of rhodopsins is boxed.

Figure 2. Conservation of the BR template in fungal rhodopsins and unique structural features of the auxiliary subgroup. CLUSTALW alignment of partial sequences of representative members of the auxiliary subgroups (highlighted purple), restricted to the conserved transmembrane regions of the last six helices (helices B-G, see supplementary file for the full-length alignment). Sequences of BR, LR, and PhaeoRD1 are given for comparison. The residues conserved in BRs are yellow on black, residues most important for proton transport are numbered using BR sequence, and the residues unique for the auxiliary group are highlighted purple. Abbreviations: Leptos. – *Leptosphaeria maculans*, Pyrenoph. – *Pyrenophora tritici-repentis*, Altern. – *Alternaria brassicicola*, Bipolar. - *Bipolaris oryzae*, Dothistr. – *Dothistroma septosporum*, Mycosph. – *Mycosphaerella graminicola*, Gibber. – *Gibberella zeae*, Fusar. – *Fusarium oxysporum*, Hyster. – *Hysterium pulicare*, Sclerot. – *Sclerotinia sclerotiorum*.

Figure 3. Characterization of the dark states of *Phaeosphaeria* rhodopsins. (Left panel) Visible spectra of solubilized purified rhodopsins at room temperature, pH 7.5. PhaeoRD1 was solubilized in 0.25% DDM, 50 mM KH_2PO_4, 400 mM NaCl, 250 mM imidazole, and PhaeoRD2 in 0.25% Triton X-100, 50 mM KH_2PO_4, 400 mM NaCl, 250 mM imidazole, 0.2 mg/ml *Pichia* lipids. (Right panel) Raman spectra of liposome-reconstituted dark-adapted rhodopsins suspended in 0.05 M KH_2PO_4, 0.1 M NaCl, pH 7, at room temperature, accumulated for 14 h with 1024 nm excitation.

Figure 4. The laser flash-induced photocycle kinetics of PhaeoRD1 in the DDM-washed yeast membranes followed by time-resolved difference spectroscopy in the visible range, measured at room temperature. The membranes were encased in polyacrylamide gels equilibrated with 0.05 M KH_2PO_4 and 0.1 M NaCl with the addition of the following buffers: pH 5 and 6 - 0.05 M MES, pH 8 - 0.05 M Tris, pH 9 - 0.05 M CHES. (Upper panel) Photocycle kinetics measured at pH 5-9 at characteristic wavelength: 620 nm – red, 540 nm – green, 460 nm – cyan, 400 nm – blue. (Lower panel) Comparison of the photocycle kinetics of PhaeoRD1 (color-coded as in the upper panel) and LR (black) at pH 6, normalized at the minimum of the 540 nm signal. The LR data are taken from the earlier multi-wavelength dataset [20].

Figure 5. The laser flash-induced photocycle kinetics of wild-type PhaeoRD2 in the DDM-washed yeast membranes followed by time-resolved difference spectroscopy in the visible range, measured at room temperature. The membranes were encased in polyacrylamide gels equilibrated with 0.05 M KH_2PO_4 and 0.1 M NaCl with the addition of the following buffers: pH 5 and 6 - 0.05 M MES, pH 8 - 0.05 M Tris, pH 9 - 0.05 M CHES. (Upper panel) Photocycle

kinetics measured at pH 5-9 at characteristic wavelength: 620 nm – red, 540 nm – green, 460 nm – cyan, 400 nm – blue. (Lower panel) Comparison of the photocycle kinetics of PhaeoRD2 (color-coded as in the upper panel) and PhaeoRD1 (black, taken from Fig. 4) at pH 6, normalized at the minimum of the 540 nm signal.

Figure 6. The laser flash-induced photocycle kinetics of PhaeoRD2 D126N mutant in yeast membranes followed by time-resolved difference spectroscopy in the visible range, measured at room temperature. The membranes (not treated with DDM) were encased in polyacrylamide gels equilibrated with 0.05 M KH_2PO_4 and 0.1 M NaCl with the addition of the following buffers: pH 5 and 6 - 0.05 M MES, pH 8 - 0.05 M Tris. (Upper panel) Photocycle kinetics measured at pH 5- 8 at characteristic wavelength: 620 nm – red, 540 nm – green, 460 nm – cyan, 400 nm – blue. (Lower panel) Comparison of the normalized photocycle kinetics at 400 nm, representing the reprotonation of the retinal Schiff base, of PhaeoRD2 wild-type (black) and the D126N mutant at pH 5 with (red) and without (blue) 1 mM NaN_3.

Figure 7. Time-resolved laser flash-induced difference FTIR spectra of *Phaeosphaeria* rhodopsins reconstituted into DMPC/DMPA liposomes hydrated with 0.05 M KH_2PO_4, 0.1 M NaCl, pH 7, and measured at 1 ms delay after the flash (but note the 12 ms full interferogram acquisition time) at 12°C. Positive bands report on the photointermediates, while the negative bands report on the dark state, the characteristic bands are marked, see text for details. (Upper panel) PhaeoRD1; (Lower panel) PhaeoRD2.

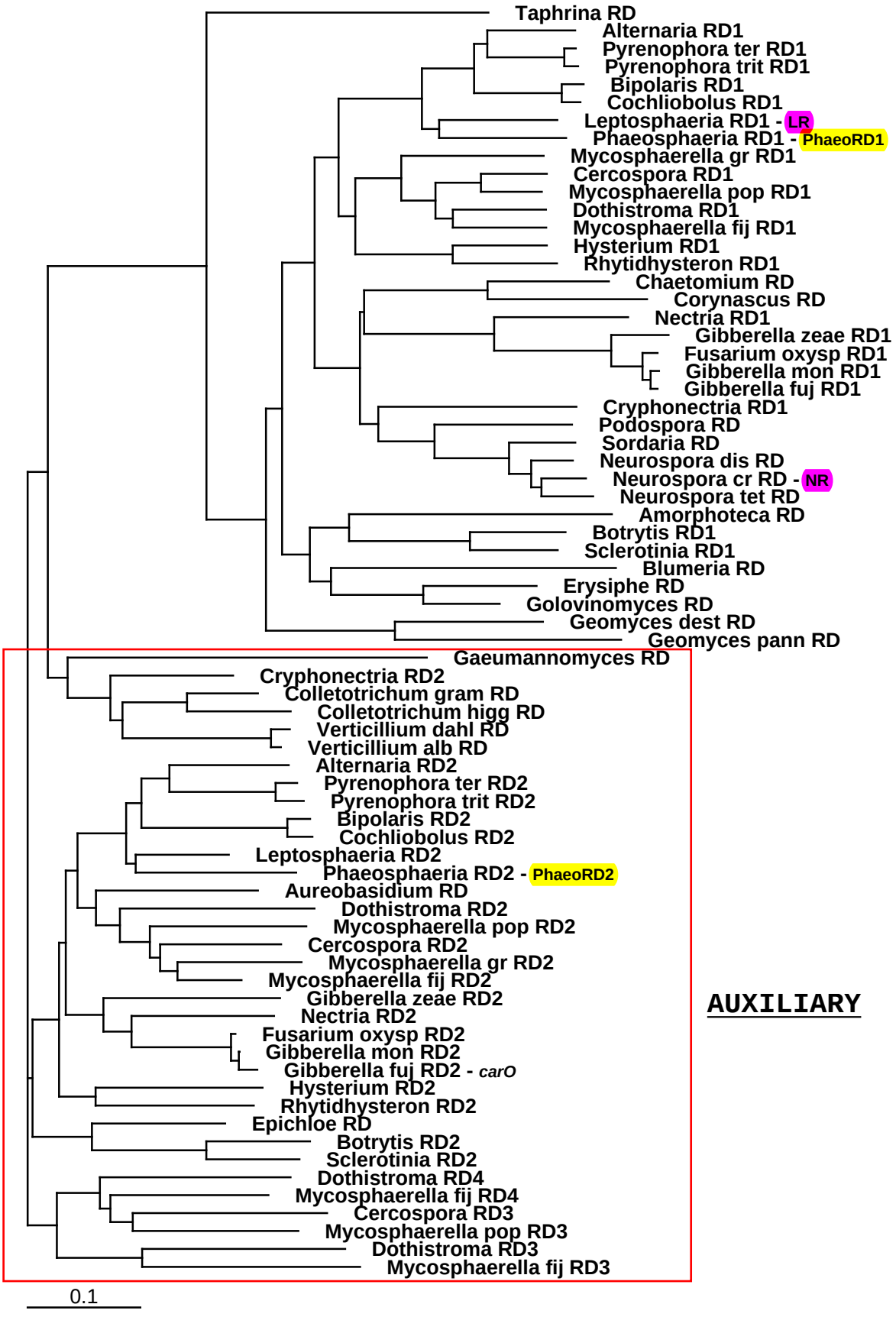
Taphrina RD
Alternaria RD1
Pyrenophora ter RD1
Pyrenophora trit RD1
Bipolaris RD1
Cochliobolus RD1
Leptosphaeria RD1 - LR
Phaeosphaeria RD1 - PhaeoRD1
Mycosphaerella gr RD1
Cercospora RD1
Mycosphaerella pop RD1
Dothistroma RD1
Mycosphaerella fij RD1
Hysterium RD1
Rhytidhysteron RD1
Chaetomium RD
Corynascus RD
Nectria RD1
Gibberella zeae RD1
Fusarium oxysp RD1
Gibberella mon RD1
Gibberella fuj RD1
Cryphonectria RD1
Podospora RD
Sordaria RD
Neurospora dis RD
Neurospora cr RD - NR
Neurospora tet RD
Amorphoteca RD
Botrytis RD1
Sclerotinia RD1
Blumeria RD
Erysiphe RD
Golovinomyces RD
Geomyces dest RD
Geomyces pann RD
Gaeumannomyces RD
Cryphonectria RD2
Colletotrichum gram RD
Colletotrichum higg RD
Verticillium dahl RD
Verticillium alb RD
Alternaria RD2
Pyrenophora ter RD2
Pyrenophora trit RD2
Bipolaris RD2
Cochliobolus RD2
Leptosphaeria RD2
Phaeosphaeria RD2 - PhaeoRD2
Aureobasidium RD
Dothistroma RD2
Mycosphaerella pop RD2
Cercospora RD2
Mycosphaerella gr RD2
Mycosphaerella fij RD2
Gibberella zeae RD2
Nectria RD2
Fusarium oxysp RD2
Gibberella mon RD2
Gibberella fuj RD2 - carO
Hysterium RD2
Rhytidhysteron RD2
Epichloe RD
Botrytis RD2
Sclerotinia RD2
Dothistroma RD4
Mycosphaerella fij RD4
Cercospora RD3
Mycosphaerella pop RD3
Dothistroma RD3
Mycosphaerella fij RD3
AUXILIARY
0.1

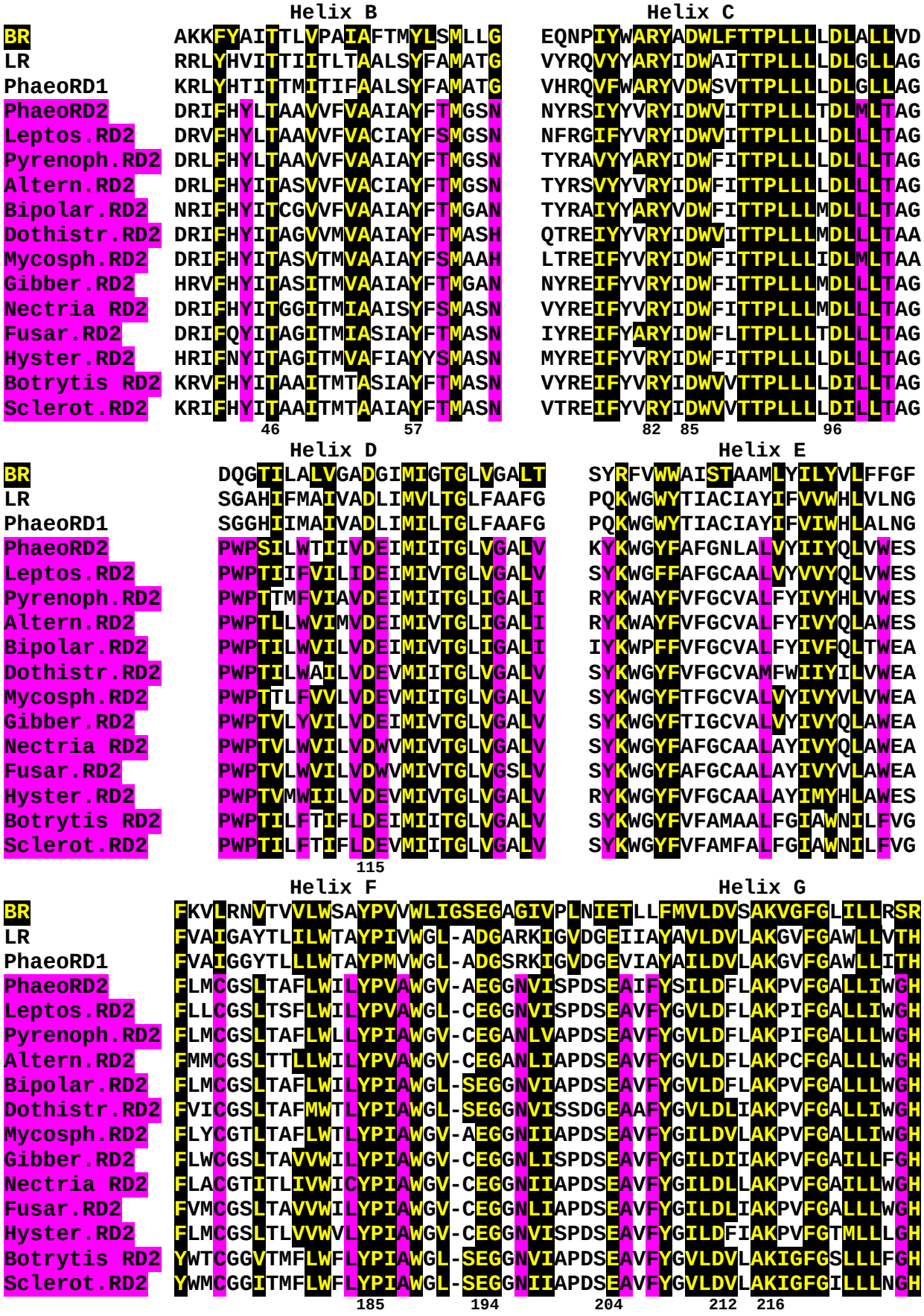
Helix B
Helix C
BR AKKFYAITTLVPAIAFTMYLSMLLG EQNPIYWARYADWLFTTPLLLLDLALLVD
LR RRLYHVITTIITLTAALSYFAMATG VYRQVYYARYIDWAITTPLLLLDLGLLAG
PhaeoRD1 KRLYHTITTMITIFAALSYFAMATG VHRQVFWARYVDWSVTTPLLLLDLGLLAG
PhaeoRD2 DRIFHYLTAAVVFVAAIAYFTMGSN NYRSIYYVRYIDWVITTPLLLTDLMLTAG
Leptos.RD2 DRVFHYLTAAVVFVACIAYFSMGSN NFRGIFYVRYIDWVITTPLLLLDLLLTAG
Pyrenoph.RD2 DRLFHYLTAAVVFVAAIAYFTMGSN TYRAVYYARYIDWFITTPLLLLDLLLTAG
Altern.RD2 DRLFHYITASVVFVACIAYFTMGSN TYRSVYYVRYIDWFITTPLLLLDLLLTAG
Bipolar.RD2 NRIFHYITCGVVFVAAIAYFTMGAN TYRAIYYARYVDWFITTPLLLMDLLLTAG
Dothistr.RD2 DRIFHYITAGVVMVAAIAYFTMASH QTREIYYVRYIDWVITTPLLLMDLLLTAA
Mycosph.RD2 DRIFHYITASVTMVAAIAYFSMAAH LTREIFYVRYIDWFITTPLLLIDLMLTAA
Gibber.RD2 HRVFHYITASITMVAAIAYFTMGAN NYREIFYVRYIDWFITTPLLLMDLLLTAG
Nectria RD2 DRIFHYITGGITMIAAISYFSMASN VYREIFYVRYIDWFITTPLLLMDLLLTAG
Fusar.RD2 DRIFQYITAGITMIASIAYFTMASN IYREIFYARYIDWFLTTPLLLTDLLLTAG
Hyster.RD2 HRIFNYITAGITMVAFIAYYSMASN MYREIFYVRYIDWFITTPLLLLDLLLTAG
Botrytis RD2 KRVFHYITAAITMTASIAYFTMASN VYREIFYVRYIDWVVTTPLLLLDILLTAG
Sclerot.RD2 KRIFHYITAAITMTAAIAYFTMASN VTREIFYVRYIDWVVTTPLLLLDILLTAG
46
57
82
85
96
Helix D
Helix E
BR DQGTILALVGADGIMIGTGLVGALT SYRFVWWAISTAAMLYILYVLFFGF
LR SGAHIFMAIVADLIMVLTGLFAAFG PQKWGWYTIACIAYIFVVWHLVLNG
PhaeoRD1 SGGHIIMAIVADLIMILTGLFAAFG PQKWGWYTIACIAYIFVIWHLALNG
PhaeoRD2 PWPSILWTIIVDEIMIITGLVGALV KYKWGYFAFGNLALVYIIYQLVWES
Leptos.RD2 PWPTIIFVILIDEIMIVTGLVGALV SYKWGFFAFGCAALVYVVYQLVWES
Pyrenoph.RD2 PWPTTMFVIAVDEIMIITGLIGALI RYKWAYFVFGCVALFYIVYHLVWES
Altern.RD2 PWPTLLWVIMVDEIMIVTGLIGALI RYKWAYFVFGCVALFYIVYQLAWES
Bipolar.RD2 PWPTILWVILVDEIMIVTGLIGALI IYKWPFFVFGCVALFYIVFQLTWEA
Dothistr.RD2 PWPTILWAILVDEVMIITGLVGALV SYKWGYFVFGCVAMFWIIYILVWEA
Mycosph.RD2 PWPTTLFVVLVDEVMIITGLVGALV SYKWGYFTFGCVALVYIVYVLVWEA
Gibber.RD2 PWPTVLYVILVDEIMIVTGLVGALV SYKWGYFTIGCVALVYIVYQLAWEA
Nectria RD2 PWPTVLWVILVDWVMIVTGLVGALV SYKWGYFAFGCAALAYIVYQLAWEA
Fusar.RD2 PWPTVLWVILVDWVMIVTGLVGSLV SYKWGYFAFGCAALAYIVYVLAWEA
Hyster.RD2 PWPTVMWIILVDEVMIVTGLVGALV RYKWGYFVFGCAALAYIMYHLAWES
Botrytis RD2 PWPTILFTIFLDEIMIITGLVGALV SYKWGYFVFAMAALFGIAWNILFVG
Sclerot.RD2 PWPTILFTIFLDEVMIITGLVGALV SYKWGYFVFAMFALFGIAWNILFVG
115
Helix F
Helix G
BR FKVLRNVTVVLWSAYPVVWLIGSEGAGIVPLNIETLLFMVLDVSAKVGFGLILLRSR
LR FVAIGAYTLILWTAYPIVWGL-ADGARKIGVDGEIIAYAVLDVLAKGVFGAWLLVTH
PhaeoRD1 FVAIGGYTLLLWTAYPMVWGL-ADGSRKIGVDGEVIAYAILDVLAKGVFGAWLLITH
PhaeoRD2 FLMCGSLTAFLWILYPVAWGV-AEGGNVISPDSEAIFYSILDFLAKPVFGALLIWGH
Leptos.RD2 FLLCGSLTSFLWILYPVAWGL-CEGGNVISPDSEAVFYGVLDFLAKPIFGALLIWGH
Pyrenoph.RD2 FLMCGSLTAFLWLLYPIAWGV-CEGANLVAPDSEAVFYGVLDFLAKPIFGALLLWGH
Altern.RD2 FMMCGSLTTLLWILYPVAWGV-CEGANLIAPDSEAVFYGVLDFLAKPCFGALLLWGH
Bipolar.RD2 FLMCGSLTAFLWILYPIAWGL-SEGGNVIAPDSEAVFYGVLDFLAKPVFGALLLWGH
Dothistr.RD2 FVICGSLTAFMWTLYPIAWGL-SEGGNVISSDGEAAFYGVLDLIAKPVFGALLIWGH
Mycosph.RD2 FLYCGTLTAFLWTLYPIAWGV-AEGGNIIAPDSEAVFYGILDVLAKPVFGALLIWGH
Gibber.RD2 FLWCGSLTAVVWILYPIAWGV-CEGGNLISPDSEAVFYGILDIIAKPVFGAILLFGH
Nectria RD2 FLACGTITLIVWICYPIAWGV-CEGGNIIAPDSEAVFYGILDLLAKPVFGAILLWGH
Fusar.RD2 FVMCGSLTAVVWILYPIAWGV-CEGGNLIAPDSEAVFYGILDLIAKPVFGALLLWGH
Hyster.RD2 FLMCGSLTLVVWVLYPIAWGV-CEGGNVISPDSEAVFYGILDFIAKPVFGTMLLLGH
Botrytis RD2 YWTCGGVTMFLWFLYPIAWGL-SEGGNVIAPDSEAVFYGVLDVLAKIGFGSLLLFGH
Sclerot.RD2 YWMCGGITMFLWFLYPIAWGL-SEGGNIIAPDSEAVFYGVLDVLAKIGFGILLLNGH
185
194
204
212
216

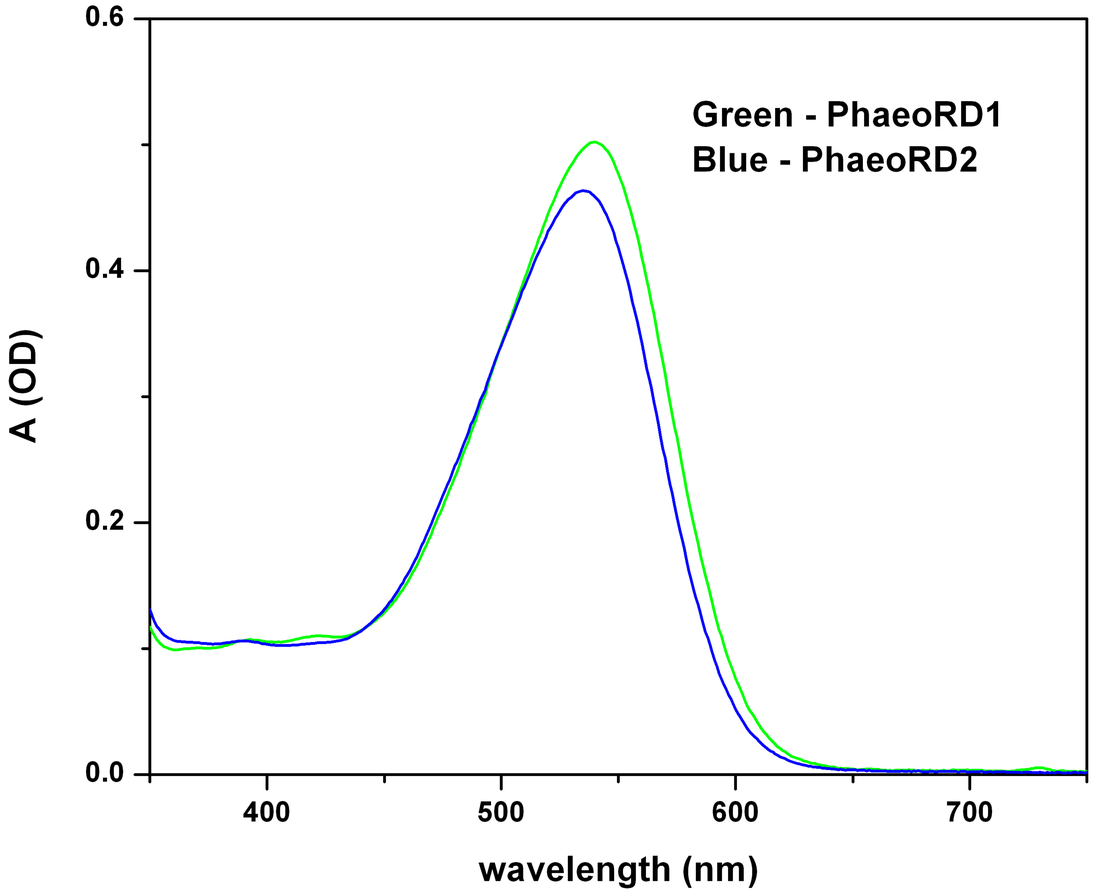
Green - PhaeoRD1
Blue - PhaeoRD2
A (OD)
0.6
0.4
0.2
0.0
400
500
600
700
wavelength (nm)

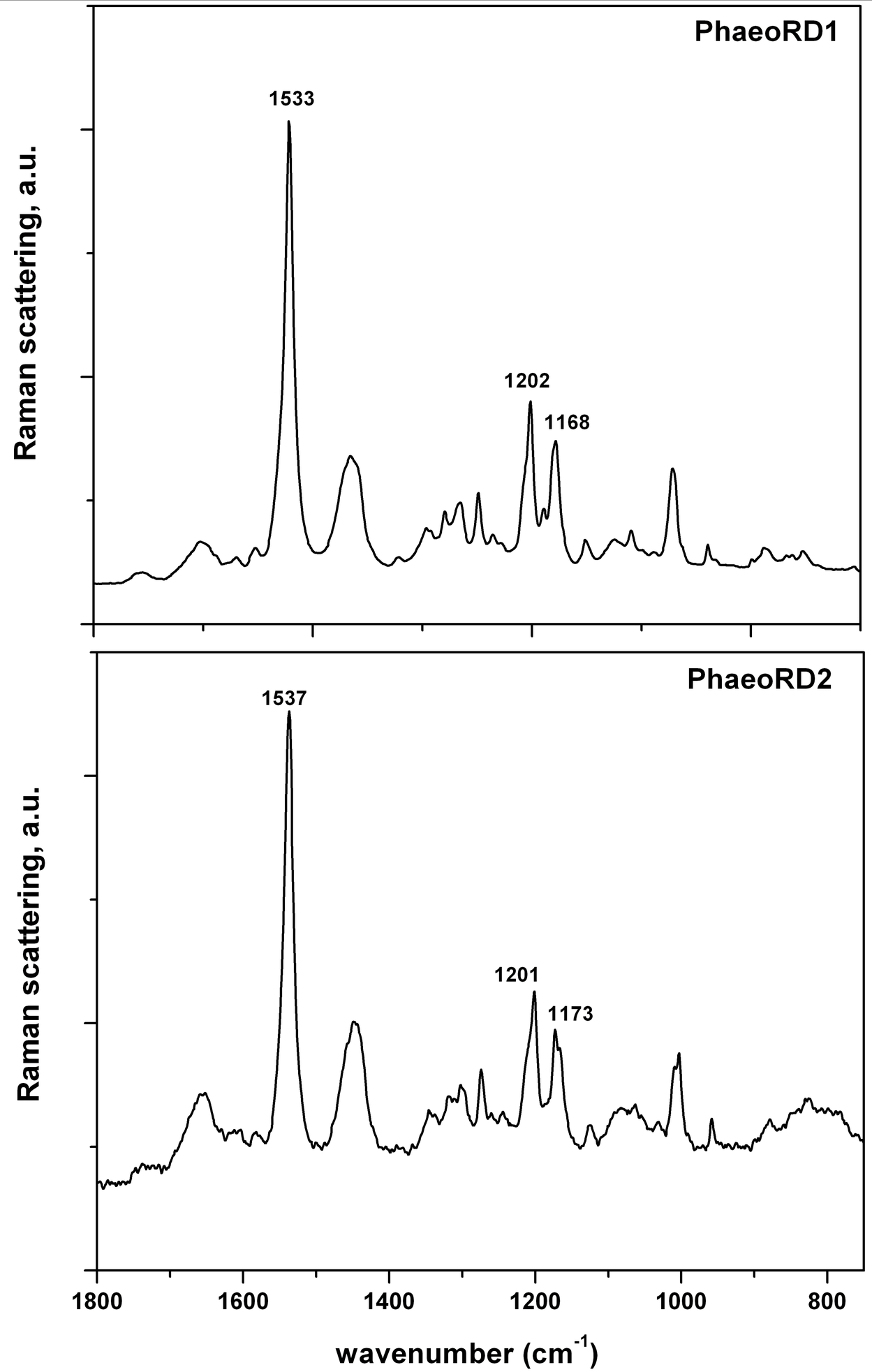
PhaeoRD1
1533
1202
1168
Raman scattering, a.u.
PhaeoRD2
1537
1201
1173
Raman scattering, a.u.
1800
1600
1400
1200
1000
800
wavenumber (cm-1)

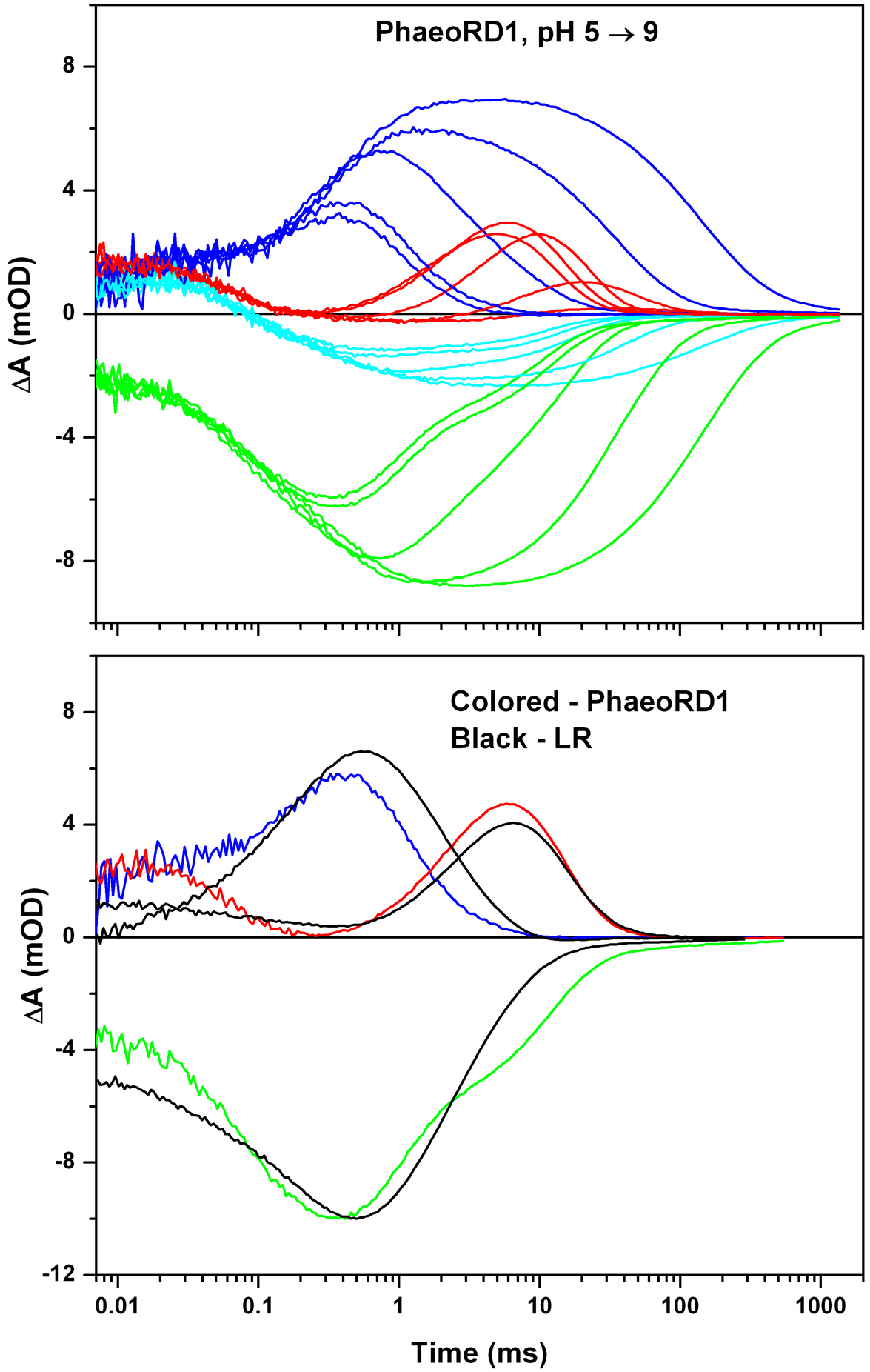
PhaeoRD1, pH 5 → 9
8
4
0
-4
-8
ΔA (mOD)
Colored - PhaeoRD1
Black - LR
8
4
0
-4
-8
-12
ΔA (mOD)
0.01
0.1
1
10
100
1000
Time (ms)

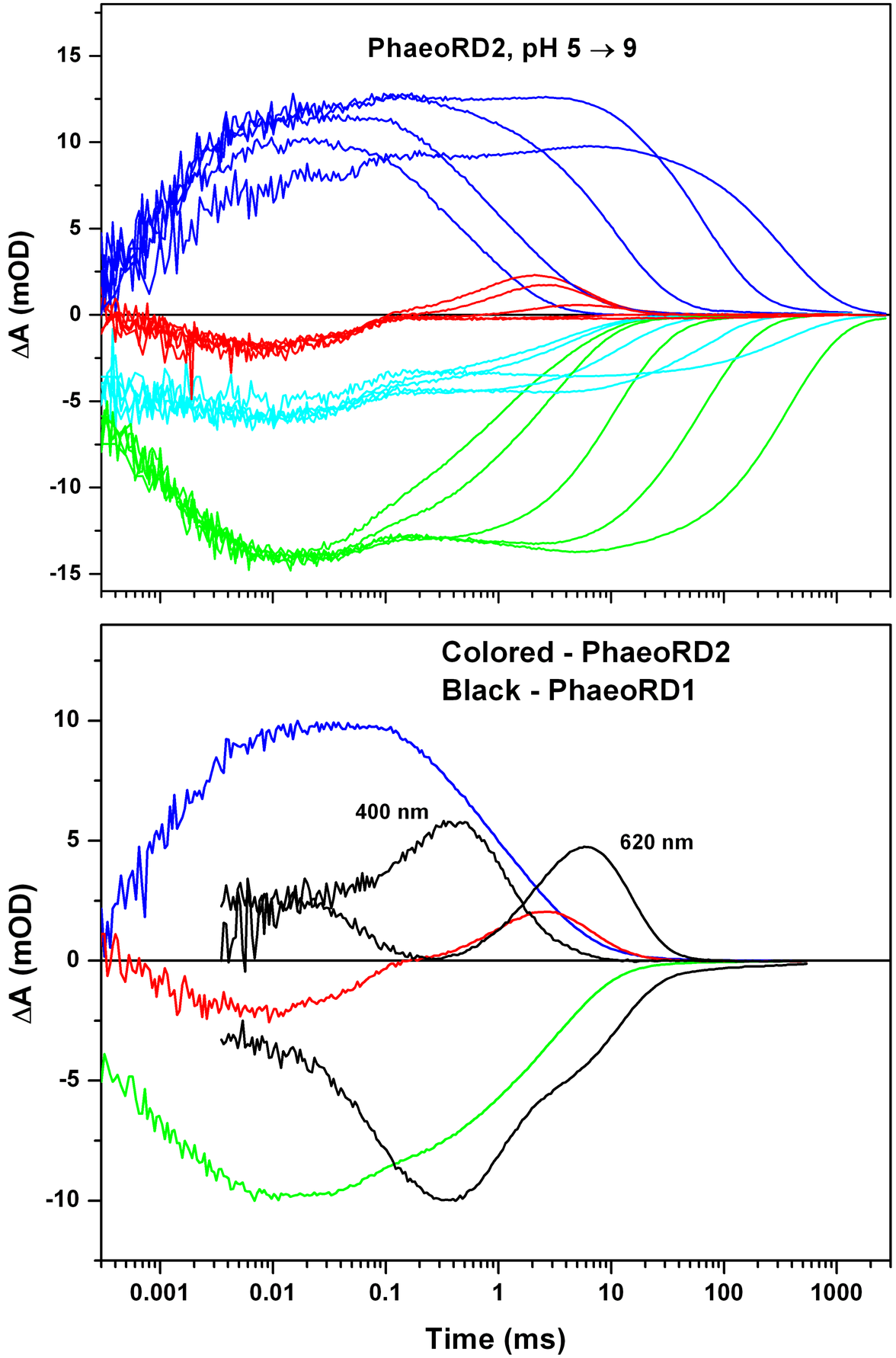
PhaeoRD2, pH 5 → 9
ΔA (mOD)
15
10
5
0
-5
-10
-15
Colored - PhaeoRD2
Black - PhaeoRD1
400 nm
620 nm
10
5
0
-5
-10
0.001
0.01
0.1
1
10
100
1000
Time (ms)

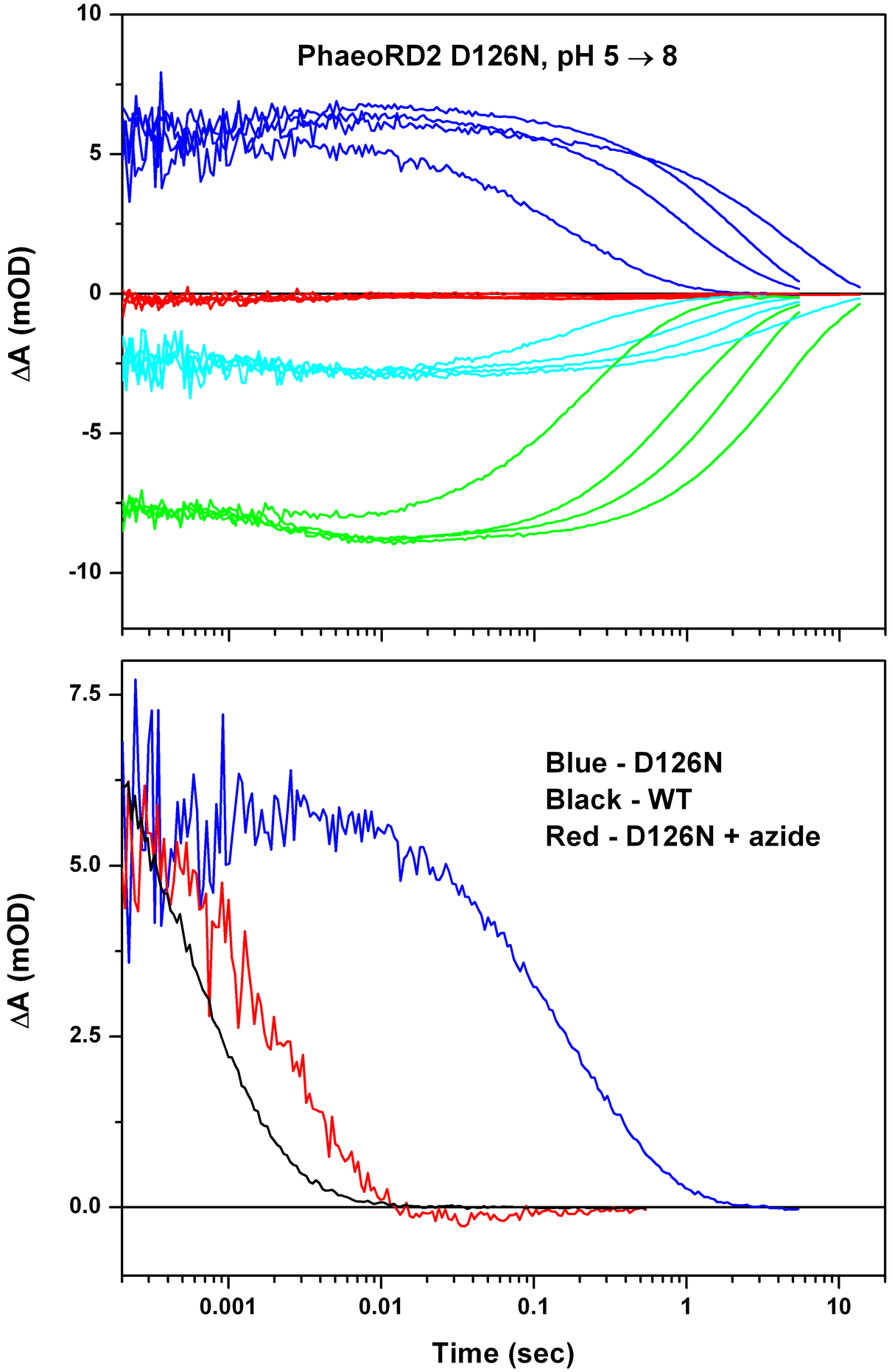
PhaeoRD2 D126N, pH 5 → 8
ΔA (mOD)
10
5
0
-5
-10
Blue - D126N
Black - WT
Red - D126N + azide
7.5
5.0
2.5
0.0
0.001
0.01
0.1
1
10
Time (sec)

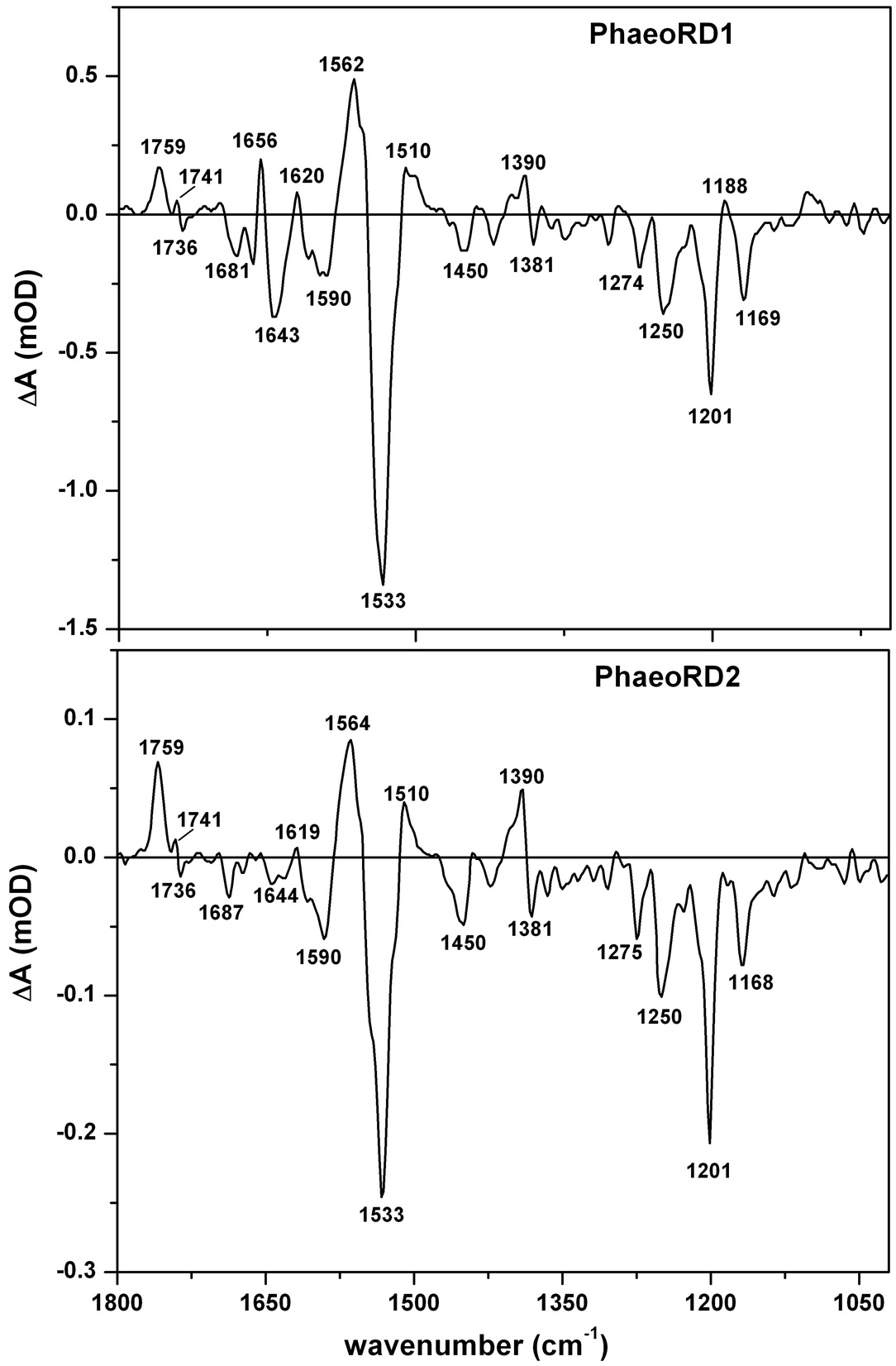
PhaeoRD1
0.5
0.0
-0.5
-1.0
-1.5
ΔA (mOD)
1759
1741
1736
1656
1681
1643
1620
1590
1562
1533
1510
1450
1390
1381
1274
1250
1188
1201
1169
PhaeoRD2
0.1
0.0
-0.1
-0.2
-0.3
1759
1741
1736
1687
1644
1619
1590
1564
1533
1510
1450
1390
1381
1275
1250
1201
1168
1800
1650
1500
1350
1200
1050
wavenumber (cm-1)

Photochemical Characterization of a novel Fungal Rhodopsin from *Phaeosphaeria nodorum*

Ying Fan[a], Peter Solomon[b], Richard P. Oliver[c], Leonid S. Brown[a,*]

[a]Department of Physics and Biophysics Interdepartmental Group, University of Guelph, Ontario, Canada, N1G 2W1; [b]Research School of Biology, College of Medicine, Biology and the Environment, The Australian National University, Canberra ACT 0200, Australia; [c]Australian Centre for Necrotrophic Fungal Pathogens, Department of Environment and Agriculture, Curtin University, GPO Box U1987, Perth, WA 6102, Australia

Supplementary data

1. Sequence alignment of rhodopsins from ascomycetes produced by CLUSTALW. Members of the auxiliary group are shown on top, LR and PhaeoRD1 are shown at the bottom for comparison.

```
                                          Helix A          Helix B
Pyrenophora_ter_RD2          RTADIAITTHGSDFYFAICSVMGFAGFAFIILGQRKARRDRLFHYLTAAV 69
Pyrenophora_trit_RD2         RTADIAITTHGSDFYFAICAVMGFAGFAFVILGQRKARRDRLFHYLTAAV 69
Alternaria_RD2               ATADIAITTHGSDFYFAICAVMGFSGFCFLGLAYRKQRRDRLFHYITASV 55
Bipolaris_RD2                RTADIGLTTHGSNFYFSICAVMTVAGFVFAAMSYRIERRNRIFHYITCGV 69
Cochliobolus_RD2             RTADIGLTTHGSDFYFSICVVMTVAGFAFAAMSYRIERRNRLFHYITCGV 69
Leptosphaeria_RD2            RTADINITSDGSSFYFAICAVMGASGFAFLFLASRRKRTDRVFHYLTAAV 45
Phaeosphaeria_RD2            RTADIAITDHGSDLYFAICAAMTVSGFVFIGLGMRKQRRDRIFHYLTAAV 70
Mycosphaerella_gr_RD2        NPPDIGITVRGSDWYWAVCAIMTVATFAFVGLSITKPRQDRIFHYITASV 68
Mycosphaerella_fij_RD2       GSAQIGITVRGSDWYWTVCAVMTVATFAFIALSATKPRQDRIFHYITAGV 53
Cercospora_RD2               ATADIALTVRGSDWYWAVCAVMTVATFAFLGMGMRKPRHDRIFHYITASV 70
Mycosphaerella_pop_RD2       GVAQIAITTHGSDFYFAVCAVMTVSTFAFLALGQMKPRAERIFYYITASV 65
Dothistroma_RD2              ATADVALTTHGSDWYWAVCAVMTCSAFAFMGLAYTKPRRDRIFHYITAGV 73
Aureobasidium_RD             KTADIAITVRGSDWYWTVCAVMTTATFVFLGLGITKPRQHRIFHYITAAI 70
Gibberella_mon_RD2           QRSDINITVRGSDWYWAVCAVMTVSTFAFLGLGMRKPRTDRIFHYITAGI 52
Gibberella_fuj_RD2           QRSDINITVRGSDWYWAVCAVMTVSTFAFLGLGMRKPRTDRIFHYITAGI 72
Fusarium_oxysp_RD2           QRSDINITVRGSDWYWAVCAVMTVSTFAFLGLGMRKPRTDRIFQYITAGI 52
Nectria_RD2                  QSSDINLTTRGSDWYWAVCAVMTVATIAFIGTAWTKPRTDRIFHYITGGI 72
Gibberella_zeae_RD2          ISTQINITPRGSDWYFTVCAVMTVSSIVFVGMGLRKPRTHRVFHYITASI 74
Hysterium_RD2                QTAEIAITVRGSDFYWAICSAMGLATLLFLAHAFTKPRSHRIFNYITAGI 69
Rhytidhysteron_RD2           RRAEIAITIRGSDFYWAICSLMGFATLCFLGLSLTKPRTHRIFHYITAGI 59
Botrytis_RD2                 ASSDISITTHGSDVYWAITAAMAFATIVFLALSFRVPRSKRVFHYITAAI 70
Sclerotinia_RD2              TSTDIAITTRGSDVYWAITAAMAFATLCFLAWSFRIPRSKRIFHYITAAI 71
Leptosphaeria_RD1            TPIYETVGDSGSKTLWVVFVLMLIASAAFTALSWKIPVNRRLYHVITTII 90
Phaeosphaeria_RD1            TPELQFIGESGQKTLWVVFVLMIIASAGFTALSWRVPLSKRLYHTITTMI 85
```

```
                                  Helix B
Pyrenophora_ter_RD2          VFVAAIAYFTMGSNLGFTPIRVEFFRSDPKVSG-----TYRAVYY 109
Pyrenophora_trit_RD2         VFVAAIAYFTMGSNLGFTPIRVEFFRDDSVVRG-----TYRAVYY 109
Alternaria_RD2               VFVACIAYFTMGSNLGFTPIAVEFARSDPKIAG-----TYRSVYY 95
Bipolaris_RD2                VFVAAIAYFTMGANLGFTPIEVEFRRSDPVVRG-----TYRAIYY 109
Cochliobolus_RD2             VFVAAIAYFTMGANLGFTPIEVEFRRNNPVVRG-----TYRAVYY 109
Leptosphaeria_RD2            VFVACIAYFSMGSNLGFTPIEVEYKRSDPVVRG-----NFRGIFY 85
Phaeosphaeria_RD2            VFVAAIAYFTMGSNLGFTPIEVEFKRNNPVVRG-----NYRSIYY 110
Mycosphaerella_gr_RD2        TMVAAIAYFSMAAHLGWTEIDVEFVRSDPRVAG-----LTREIFY 108
Mycosphaerella_fij_RD2       TMVAAIAYFTMGSHLGFTPIDVEFARSGPKVAG-----VNREIYY 93
Cercospora_RD2               TMVAAIAYFSMGSHLGWTPINVEFERSDPRVAG-----LNREIYY 110
Mycosphaerella_pop_RD2       TMVAAIAYFTMGSHLGFTPIDVEYQRSNSRVAG-----VNREIYY 105
Dothistroma_RD2              VMVAAIAYFTMASHLGWTPIVIEFQRSNPVVRG-----QTREIYY 113
Aureobasidium_RD             TMVAAIAYFSMGSNLGWTPIDVEFSRNNPVVRG-----VNREIFY 110
Gibberella_mon_RD2           TMIASIAYFTMASNLGWTPIAVEFQRSDHRVAG-----IYREIFY 92
Gibberella_fuj_RD2           TMIASIAYFTMASNLGWTPIAVEFQRSNHRVAG-----IYREIFY 112
Fusarium_ oxysp_RD2          TMIASIAYFTMASNLGWTPIAVEFQRSDHRVAG-----IYREIFY 92
Nectria_RD2                  TMIAAISYFSMASNLGWTPIAVQFRRSDHRVAG-----VYREIFY 112
Gibberella_zeae_RD2          TMVAAIAYFTMGANLGWAPTEVEFHRRDHEVAG-----NYREIFY 114
Hysterium_RD2                TMVAFIAYYSMASNLGWTPIQVEYQRSDHRVSG-----MYREIFY 109
Rhytidhysteron_RD2           TMVAFIAYFSMAANLGWVPIAVEFSRSDPKVAG-----AYREIFY 99
Botrytis_RD2                 TMTASIAYFTMASNLGYASIIQEFQRSDPKVSG-----VYREIFY 110
Sclerotinia_RD2              TMTAAIAYFTMASNLGYASIIQEFQRGNPKVRG-----VTREIFY 111
Leptosphaeria_RD1            TLTAALSYFAMATGHGVALNKIVI-RTQHDHVPDTYETVYRQVYY 134
Phaeosphaeria_RD1            TIFAALSYFAMATGHGVSVQKIIV-REQHDHVPDTFTEVHRQVFW 129

                             Helix C                        Helix D
Pyrenophora_ter_RD2          ARYIDWFITTPLLLLDLLLTAGTPWPTTLFVIAIDEIMIVTGLIGALVD 158
Pyrenophora_trit_RD2         ARYIDWFITTPLLLLDLLLTAGTPWPTTMFVIAVDEIMIITGLIGALID 158
Alternaria_RD2               VRYIDWFITTPLLLLDLLLTAGMPWPTLLWVIMVDEIMIVTGLIGALID 144
Bipolaris_RD2                ARYVDWFITTPLLLMDLLLTAGMPWPTILWVILVDEIMIVTGLIGALIQ 158
Cochliobolus_RD2             ARYVDWFITTPLLLMDLLLTAGMPWPTILWVILVDEIMIVTGLIGALIQ 158
Leptosphaeria_RD2            VRYIDWVITTPLLLLDLLLTAGMPWPTIIFVILIDEIMIVTGLVGALVV 134
Phaeosphaeria_RD2            VRYIDWVITTPLLLTDLMLTAGMPWPSILWTIIVDEIMIITGLVGALVT 159
Mycosphaerella_gr_RD2        VRYIDWFITTPLLLIDLMLTAAMPWPTTLFVVLVDEVMIITGLVGALVS 157
Mycosphaerella_fij_RD2       VRYIDWFITTPLLLMDLMLTAAMPWPTTAWVILVDEVMIITGLVGALVS 142
Cercospora_RD2               VRYIDWFITTPLLLADLMLTAAMPWPTTAFVILVDEVMIITGLVGALVS 159
Mycosphaerella_pop_RD2       ARYIDWVITTPLLLIDLMLTAAMPWPSILFVILVDEVMIITGLIGALVA 154
Dothistroma_RD2              VRYIDWVITTPLLLMDLLLTAAMPWPTILWAILVDEVMIITGLVGALVA 162
Aureobasidium_RD             VRYIDWFITTPLLLMDLLLTAAMPWPTLLFVVLVDEVMIVTGLVGALVR 159
Gibberella_mon_RD2           ARYIDWFLTTPLLLTDLLLTAGMPWPTVLWVILVDWVMIVTGLVGALVK 141
Gibberella_fuj_RD2           ARYIDWFLTTPLLLTDLLLTAGMPWPTVLWVILVDWVMIVTGLVGALVK 161
Fusarium_ oxysp_RD2          ARYIDWFLTTPLLLTDLLLTAGMPWPTVLWVILVDWVMIVTGLVGSLVK 141
Nectria_RD2                  VRYIDWFITTPLLLMDLLLTAGMPWPTVLWVILVDWVMIVTGLVGALVK 161
Gibberella_zeae_RD2          VRYIDWFITTPLLLMDLLLTAGMPWPTVLYVILVDEIMIVTGLVGALVT 163
Hysterium_RD2                VRYIDWFITTPLLLLDLLLTAGMPWPTVMWIILVDEVMIVTGLVGALVR 158
Rhytidhysteron_RD2           VRYIDWFITTPLLLLDLLLTAGMPWPTVLWVILVDWAMIVTGLVGALVQ 148
Botrytis_RD2                 VRYIDWVVTTPLLLLDILLTAGLPWPTILFTIFLDEIMIITGLVGALVA 159
Sclerotinia_RD2              VRYIDWVVTTPLLLLDILLTAGLPWPTILFTIFLDEVMIITGLVGALVA 160
Leptosphaeria_RD1            ARYIDWAITTPLLLLDLGLLAGMSGAHIFMAIVADLIMVLTGLFAAFGS 183
Phaeosphaeria_RD1            ARYVDWSVTTPLLLLDLGLLAGMSGGHIIMAIVADLIMILTGLFAAFGE 178
```

```
                                  Helix E                                 Helix F
Pyrenophora_ter_RD2          --NRYKWAYFVFGCVALFYIVYHLVWESRLQAKKFGRDVERCFLMCGSLT 206
Pyrenophora_trit_RD2         --NRYKWAYFVFGCVALFYIVYHLVWESRLQAKKFGRDVERCFLMCGSLT 206
Alternaria_RD2               --NRYKWAYFVFGCVALFYIVYQLAWESRIHAKSFGRDVERTFMMCGSLT 192
Bipolaris_RD2                --SIYKWPFFVFGCVALFYIVFQLTWEARIHSKTFGRDVERTFLMCGSLT 206
Cochliobolus_RD2             --SIYKWPFFVFGCAALFYIVFQLTWEARIHSKTFGRDVERTFLMCGSLT 206
Leptosphaeria_RD2            --SSYKWGFFAFGCAALVYVVYQLVWESRRHSKFFGRDVERTFLLCGSLT 182
Phaeosphaeria_RD2            --SKYKWGYFAFGNLALVYIIYQLVWESRTHARHFGRDVERTFLMCGSLT 207
Mycosphaerella_gr_RD2        --SSYKWGYFTFGCVALVYIVYVLVWEARKHANGVSSDAGKAFLYCGTLT 205
Mycosphaerella_fij_RD2       --SSYKWGYFVFGCVALIWIVYVLVWEARKHAYGVSSDAGKAFMFCGSLT 190
Cercospora_RD2               --SSYKWGYFTFGCVALGYIVYVLAWEARLHANGISSDAGKAFLYCGSLT 207
Mycosphaerella_pop_RD2       --SSYKWGYFVFGCVALVYIVYVLVWEARKHANGVSSDAGKTFLYCGSLT 202
Dothistroma_RD2              --SSYKWGYFVFGCVAMFWIIYILVWEARIHANAISTDAGRAFVICGSLT 210
Aureobasidium_RD             --SSYKWGYFVFGCVALFYVVWVLVWEARRHANALGSDVGRAFTICGSLT 207
Gibberella_mon_RD2           --SSYKWGYFAFGCAALAYIVYVLAWEARLHAKHVGPDVGRTFVMCGSLT 189
Gibberella_fuj_RD2           --SSYKWGYFAFGCAALAYIVYVLAWEARLHAKHVGPDVGRTFVMCGSLT 209
Fusarium_ oxysp_RD2          --SSYKWGYFAFGCAALAYIVYVLAWEARLHAKHVGPDVGRTFVMCGSLT 189
Nectria_RD2                  --SSYKWGYFAFGCAALAYIVYQLAWEARIHANRIGNDVGRVFLACGTIT 209
Gibberella_zeae_RD2          --TSYKWGYFTIGCVALVYIVYQLAWEARIHANHVGPDVGRVFLWCGSLT 211
Hysterium_RD2                --TRYKWGYFVFGCAALAYIMYHLAWESRRNASRLGNDIGRVFLMCGSLT 206
Rhytidhysteron_RD2           --SRYKWGYFTFGCVALFYIIYQLAWEARRHATKLGEDVGRAFLYCGSLT 196
Botrytis_RD2                 --SSYKWGYFVFAMAALFGIAWNILFVGAQHAKALGSEVNKVYWTCGGVT 207
Sclerotinia_RD2              --SSYKWGYFVFAMFALFGIAWNILFVGARHAKSLGTEVNKTYWMCGGIT 208
Leptosphaeria_RD1            EGTPQKWGWYTIACIAYIFVVWHLVLNGGANARVKGEKLRSFFVAIGAYT 233
Phaeosphaeria_RD1            EGTPQKWGWYTIACIAYIFVIWHLALNGGANATSKGPKLRSFFVAIGGYT 228

                             Helix F                      Helix G
Pyrenophora_ter_RD2          AFLWILYPIAWGICEGANLIAPDSEAVFYGVLDFLAKPIFGALLLWGHR 255
Pyrenophora_trit_RD2         AFLWLLYPIAWGVCEGANLVAPDSEAVFYGVLDFLAKPIFGALLLWGHR 255
Alternaria_RD2               TLLWILYPVAWGVCEGANLIAPDSEAVFYGVLDFLAKPCFGALLLWGHK 241
Bipolaris_RD2                AFLWILYPIAWGLSEGGNVIAPDSEAVFYGVLDFLAKPVFGALLLWGHR 255
Cochliobolus_RD2             AFLWILYPVAWGLSEGGNVIAPDSEAVFYGVLDFLAKPVFGALLLWGHR 255
Leptosphaeria_RD2            SFLWILYPVAWGLCEGGNVISPDSEAVFYGVLDFLAKPIFGALLIWGHR 231
Phaeosphaeria_RD2            AFLWILYPVAWGVAEGGNVISPDSEAIFYSILDFLAKPVFGALLIWGHR 256
Mycosphaerella_gr_RD2        AFLWTLYPIAWGVAEGGNIIAPDSEAVFYGILDVLAKPVFGALLIWGHR 254
Mycosphaerella_fij_RD2       ALLWTLYPIAWGVSEGGNVIAPDSEAVFYGILDILAKPGFGALLLWGHR 239
Cercospora_RD2               AFLWILYPIAWGVCEGGNVIAVDSEAVFYGILDLLAKPVFGALLIWGHR 256
Mycosphaerella_pop_RD2       AFLWILYPVAWGVSEGGNIIAPDSEAVFYGILDLLAKPLFGALLIWGHR 251
Dothistroma_RD2              AFMWTLYPIAWGLSEGGNVISSDGEAAFYGVLDLIAKPVFGALLIWGHR 259
Aureobasidium_RD             TFLWILYPLAWGLCEGGNVISPDSEAIFYGILDLLAKPVFGALLIWGHR 256
Gibberella_mon_RD2           AVVWILYPIAWGVCEGGNLIAPDSEAVFYGILDLIAKPVFGALLLWGHR 238
Gibberella_fuj_RD2           AVVWILYPIAWGVCEGGNLIAPDSEAVFYGILDLIAKPVFGALLLWGHR 258
Fusarium_ oxysp_RD2          AVVWILYPIAWGVCEGGNLIAPDSEAVFYGILDLIAKPVFGALLLWGHR 238
Nectria_RD2                  LIVWICYPIAWGVCEGGNIIAPDSEAVFYGILDLLAKPVFGAILLWGHR 258
Gibberella_zeae_RD2          AVVWILYPIAWGVCEGGNLISPDSEAVFYGILDIIAKPVFGAILLFGHR 260
Hysterium_RD2                LVVWVLYPIAWGVCEGGNVISPDSEAVFYGILDFIAKPVFGTMLLLGHR 255
Rhytidhysteron_RD2           LVLWICYPIAWGVCEGGNVIAPDSEAVFYGVLDFLAKPVFGALLMFGHR 245
Botrytis_RD2                 MFLWFLYPIAWGLSEGGNVIAPDSEAVFYGVLDVLAKIGFGSLLLFGHR 256
Sclerotinia_RD2              MFLWFLYPIAWGLSEGGNIIAPDSEAVFYGVLDVLAKIGFGILLLNGHR 257
Leptosphaeria_RD1            LILWTAYPIVWGLADGARKIGVDGEIIAYAVLDVLAKGVFGAWLLVTHA 282
Phaeosphaeria_RD1            LLLWTAYPMVWGLADGSRKIGVDGEVIAYAILDVLAKGVFGAWLLITHA 277
```

```
Pyrenophora_ter_RD2          DIDPARLGLAIRDYDG-DAVVHEKVKP-------AQNHSAAPP--VDATV 295
Pyrenophora_trit_RD2         DIDPARLGLAIRDYDG-DAVVHEKVKP-------AQNHSAAPP--VDATV 295
Alternaria_RD2               GIDPARLGLSITDYDG-DAMVHEKRNPN----TVNNDQTATHPDGYNGTA 286
Bipolaris_RD2                NIDPARLGLQIRDYND-DTMLQEKRAKD----AAAHNGQNVVNPPHDGPA 300
Cochliobolus_RD2             NIDPARLGLQIRDYND-DTMLQEKRVKD----AAAHNGQNVVNPPHDGPA 300
Leptosphaeria_RD2            NVDPARLGLAIRDYGDADAVVHEKRAP-----------AVHPDGPINN  240
Phaeosphaeria_RD2            NIDPARLGLAIKDYDH-DTSVSEKRKPD-----VAPGTTAAHNPPLDGPA 300
Mycosphaerella_gr_RD2        NISPAQLGLTIRDYNGTDAVIHEKRTGV----ANGNTSNVTHENAAAN-- 298
Mycosphaerella_fij_RD2       NISPAQLGLSIRDYDGTDPVIHEKR----------------------- 264
Cercospora_RD2               NITPAQLGLTIHDYGGDDPVVHHEKSAG----APGHTGHPSENPALHNNG 302
Mycosphaerella_pop_RD2       NISPAQLGLTIHDYGGEDPVIHEKNTGI----SHGHTGHPGDNPANVGVM 297
Dothistroma_RD2              NISPADLGLAIHDYGADEPIFHEKNHRN----GNGPLADHSGATRPINSA 305
Aureobasidium_RD             GIDPARLGLYIHDYDEKDPAVKDKVG------APGPNVHPNTNNAAAT-- 298
Gibberella_mon_RD2           NIDPARLGLRIRDIDER-IFPDGP----------NNKAASGHGARNDTA- 276
Gibberella_fuj_RD2           NIDPARLGLRIRDIDER-IFPDGP----------NNKVASGHGARNDTAT 297
Fusarium_ oxysp_RD2          NIDPARLGLRIRDIDER-IFPDGP----------NNKATSGHGARNDTA- 276
Nectria_RD2                  NIDPARLGLRIRDVTEGPVYPEGPGAQK----RSVNEPAVGAGANGTQNP 304
Gibberella_zeae_RD2          NIDPARLGLRIRDVNER-IVPEGP----------NVKPGQQRNAGNVNAP 299
Hysterium_RD2                NIDPARLGLQIRDYDEDLSVHGGL----------GRGEKRTPNAPLDGPA 295
Rhytidhysteron_RD2           NIDPGRLGLRIRDYDEDPSIHGGVSGREKALHQNGTNEAQAVGGVTDGAT 295
Botrytis_RD2                 NIDPAHLGLHIRDYNEQPRTFNDKDVGHHNGAHHDGAHVPVTNNGYREGQ 306
Sclerotinia_RD2              NIDPAHLGLHIRDYNEQPGSFHEKNS-YANGAAGS-SSAPVTG------- 298
Leptosphaeria_RD1            NLRESDVELNGFWANGLNREGAIRIGEDDGA------------------- 313
Phaeosphaeria_RD1            KLRESDVELNGFWSNGLNSEGAVRLGEDDGA------------------- 308
```

2. Supplementary figures

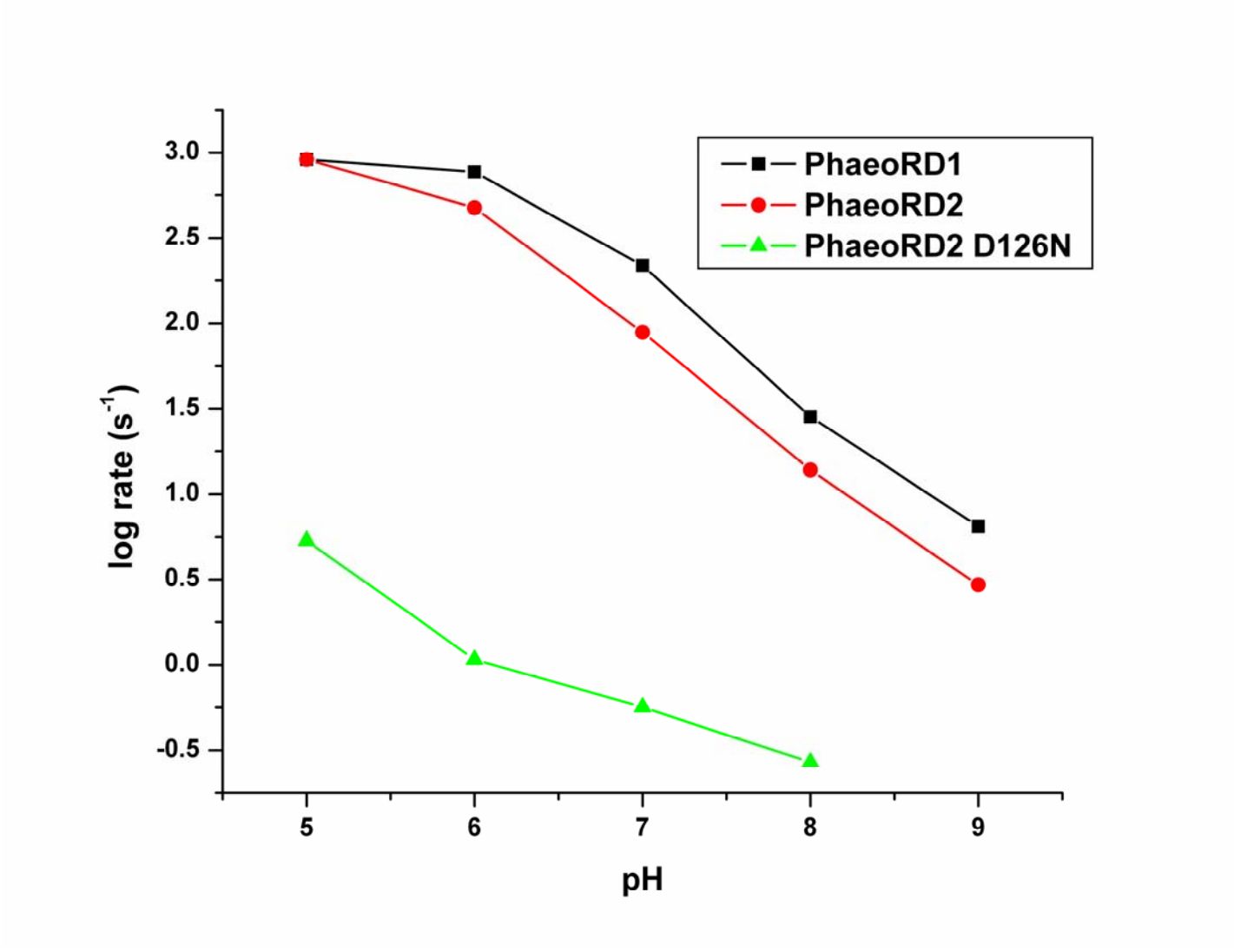

Figure S1. pH-dependence of the rates of reprotonation of the Schiff base (M decay) obtained by the exponential fitting of the data shown in Figs. 4-6.

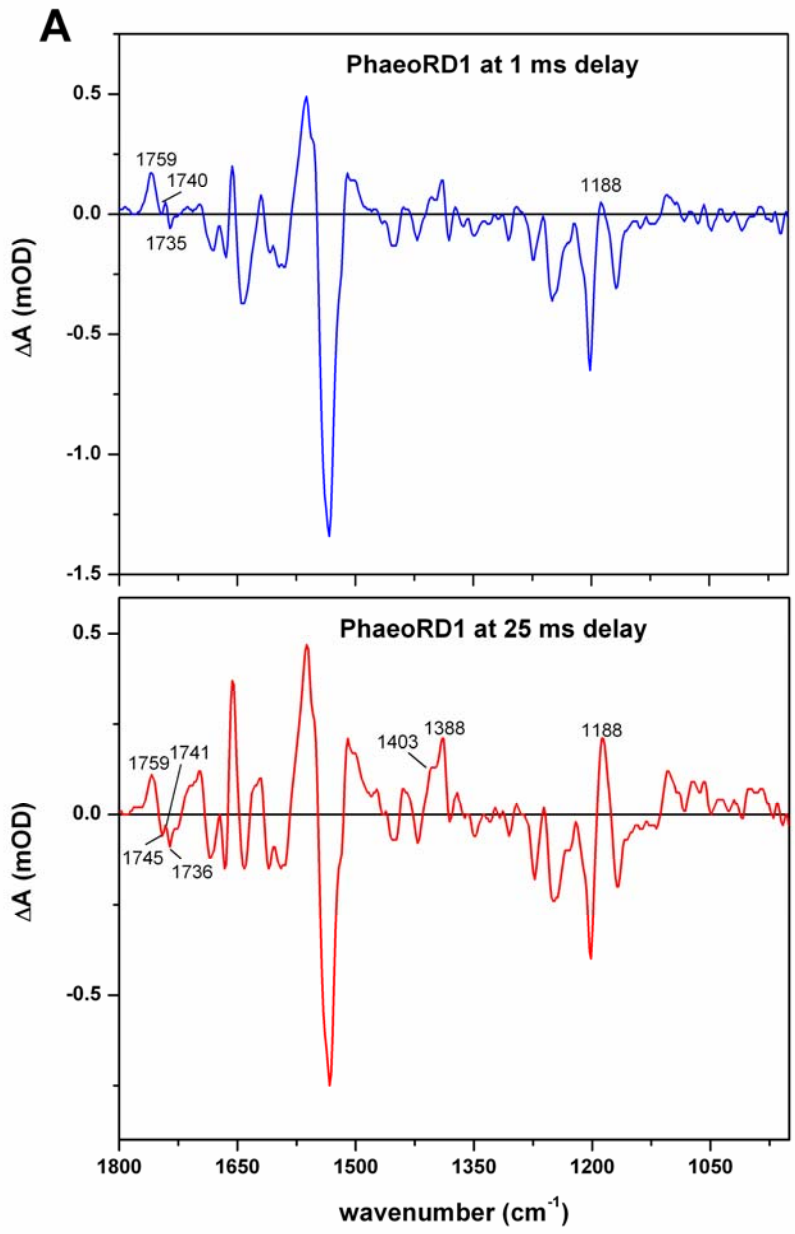
A
PhaeoRD1 at 1 ms delay
1759
1740
1735
1188
PhaeoRD1 at 25 ms delay
1759
1741
1745
1736
1403
1388
1188
ΔA (mOD)
0.5
0.0
-0.5
-1.0
-1.5
1800
1650
1500
1350
1200
1050
wavenumber (cm-1)

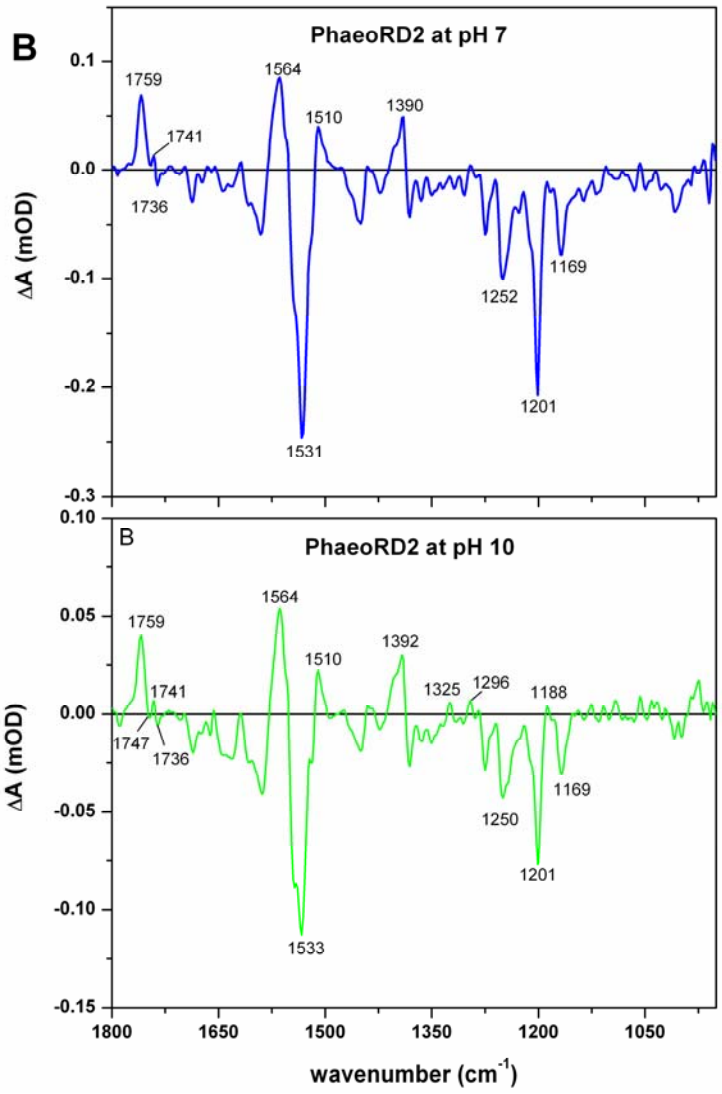

Figure S2. Time-resolved laser flash-induced difference FTIR spectra of *Phaeosphaeria* rhodopsins reconstituted into DMPC/DMPA liposomes under the conditions promoting accumulation of the late intermediates. Difference spectra of the mixtures dominated by the M intermediates from Fig. 7 are given for the comparison. Positive bands report on the photointermediates, while the negative bands report on the dark state, the characteristic bands are marked, see the text for details. (A) PhaeoRD1 liposomes hydrated with 0.05 M KH_2PO_4, 0.1 M NaCl, pH 7, and measured at 1 ms (upper panel, from Fig. 7) and 25 ms (lower panel) delays after the flash (but note the 12 ms full interferogram acquisition time) at 12°C. (B) PhaeoRD2 liposomes measured at 1 ms delay after the flash, hydrated with 0.05 M KH_2PO_4, 0.1 M NaCl, pH 7 (upper panel, from Fig. 7) and with 0.05 M KH_2PO_4, 0.1 M NaCl, 0.05 M CHES, pH 10 (lower panel).